Journal of Geochemical Exploration 278 (2025) 107857

Contents lists available at ScienceDirect

Journal of Geochemical Exploration

journal homepage: www.elsevier.com/locate/gexplo

Multivariate compositional analysis of groundwater geochemistry in the Georgina Basin: New insights for sediment-hosted mineral systems

Ivan Frederick Schroder [a,*], Patrice de Caritat [a,b], David Huston [a,c], David Champion [a,d]

[a] Geoscience Australia, GPO Box 378, Canberra, ACT 2601, Australia
[b] John de Laeter Centre, Curtin University, Bentley, WA 6102, Australia
[c] Research School of Earth Sciences, Australian National University, Acton, ACT 2601, Australia
[d] Granite Resources, PO Box 45, Gungahlin, ACT 2913, Australia

ARTICLE INFO

Keywords:
Groundwater chemistry
Mineral exploration
Phosphate
Sediment-hosted
Georgina Basin
K-means clustering
Pb isotopes

ABSTRACT

The Georgina Basin in northern Australia holds significant potential for strategic minerals, particularly zinc and phosphate, which are crucial for Australia's economy and transition to net-zero. This study applied multivariate statistical tools to groundwater geochemistry from the basin's regional Cambrian Limestone Aquifer to investigate the prospectivity of sediment-hosted phosphate and Zn–Pb mineral systems in the northern half of the Georgina Basin. Robust principal component analysis (rPCA) identified Mo and I^- (as well as Rb and Al) as key elements associated with the variation of P in groundwater. K-means cluster analysis then mapped a subset of spatial clusters where these P relationships were evident. This investigation culminated in the creation of a new geochemical index (*Phos#*) for identifying hydrogeochemical anomalies likely sourced from phosphate mineralisation. Five areas were deemed most prospective using *Phos#*: three near Elliott, and one in each of the Central Georgina and Undilla Sub-basins.

The hydrogeochemistry was also valuable in detecting regional sediment-hosted Zn–Pb mineralisation. Radiogenic Pb-isotope outliers ($^{206}Pb/^{204}Pb$ of 22.00 to 24.00) in the Alexandria-Wonarah Basement High and Undilla Sub-basin (which were supported by elevated Pb or Zn in groundwater), were spatially correlated with observed sulfides at the surface or in drillholes and consistent with the radiogenic Pb-isotope signature of Georgina Basin's Joplin-type, Mississippi Valley Type Zn–Pb mineralisation.

This regional in-depth assessment of the groundwater chemistry provides an efficient scale-reduction tool with clear targets for follow-up, and is supported by a discussion on how this multivariate, index-based approach can be translated to other sedimentary basins and/or mineralisation assemblages.

1. Introduction

The continuation of Australia's commodity pipeline, with a focus on critical minerals and strategic materials, is crucial to maintaining prosperity and enabling the country's transition to net-zero. Zinc and phosphate are both strategic minerals (Critical Minerals Office, 2024), the former for its galvanising properties in construction and transport industries, the latter for its use in fertilisers and animal feed (Hughes et al., 2025). Both Zn and phosphate can occur in sedimentary basins as sediment-hosted mineral systems. The Georgina Basin of northern Australia has known Zn–Pb and phosphate sediment-hosted mineral deposits but is under-explored for these commodities (Kruse et al., 2013). Georgina Basin phosphates have received moderate attention due to outcropping mineralisation on the eastern and southern margins of the basin (Kruse et al., 2013). However, despite the prospective geology continuing deeper into the basin (Dixon-Jain et al., 2024), our understanding of phosphate mineralisation beyond the basin margins is lacking (Dunster and Munson, 2017). Similarly, what is known about the sediment-hosted Zn–Pb is largely based on outcropping deposits in the basin's southern margins, with only a couple of occurrences documented in the central and northern part of the basin (Kruse et al., 2013).

Renewed focus for these mineral systems is warranted based on recent insights. Valetich et al. (2022) demonstrated that the rare earth element (REE) enrichment of Georgina Basin phosphates can be much higher than previously thought, highlighting the potential of new and existing phosphate deposits for REEs. In addition, Cloutier et al. (2023)

* Corresponding author.
E-mail address: ivan.schroder@ga.gov.au (I.F. Schroder).

https://doi.org/10.1016/j.gexplo.2025.107857
Received 21 January 2025; Received in revised form 20 June 2025; Accepted 28 June 2025
Available online 4 July 2025

have modelled national prospectivity of sediment hosted Zn–Pb systems and suggested much of the Georgina Basin as moderately to highly prospective.

To better explore for these mineral systems and assess their prospectivity under cover, novel or unconventional paradigms are needed, such as exploiting the advantages of groundwater geochemistry. Groundwater chemistry is the culmination of a series of chemical reactions between it and minerals in the hosting aquifer (e.g. mineral dissolution, ion exchange, leaching, weathering), across different temporal and spatial scales (Elango and Kannan, 2007), meaning the groundwater can give us insights into the subsurface geology. Looking at the groundwater geochemistry regionally can be a useful part of the exploration toolkit for identifying compositional changes in the aquifer geology or more discrete geochemical anomalies relating to mineralisation, which can inform area selection as an exploration scale-reduction tool (Leybourne and Cameron, 2010). The elemental and isotopic composition of groundwater (collectively referred to as hydrogeochemistry) has been used to explore for a range of deposit types globally including sediment-hosted base-metals, Au, volcanic-hosted massive sulfides, porphyry Cu, sediment-hosted U, alkali brines, and phosphate (e.g. Caritat et al., 2005, Ariunbileg et al., 2016, Gray et al., 2018, Kidder et al., 2022, Leybourne and Cameron, 2010, Reid et al., 2021). The advantage of hydrogeochemistry as a regional exploration tool is that it can detect geochemical anomalies related to mineralisation extending laterally for far greater distances than the geological deposits and their alteration haloes (Caritat and Kirste, 2005b). Like more typical exploration geochemistry, hydrogeochemical anomalies are also not restricted to the commodity elements of interest but include associated pathfinder elements and a range of isotope systems that can be combined in geochemical indices.

The use of isotopes in hydrogeochemistry for mineral exploration is a growing research space, given the sensitivity and level of discrimination isotopes can provide to subsurface mineralisation sources. A host of 'new' metal isotopes are being investigated for their potential in groundwater and mineral systems, including Mo, Cu, Zn, and Fe (Kidder et al., 2021; Mahan et al., 2023; Mathur and Wang, 2019; Mathur and Zhao, 2023; Tao et al., 2022). Established hydrogeochemical isotope systems that can be applied to mineral systems include S, Sr and Pb. Sulfur isotopes ($\delta^{34}S_{SO4}$) are valuable for fingerprinting sulfur sources and oxidation pathways (e.g. Caritat et al., 2005, Kidder et al., 2021). Strontium isotopes ($^{87}Sr/^{86}Sr$) are used extensively for understanding host-rock lithology, constraining water-rock interactions (WRIs) and understanding hydrogeological processes (e.g. Kidder et al., 2021; Moya et al., 2016). Lead isotopes ($^{206}Pb/^{204}Pb$, $^{207}Pb/^{204}Pb$, $^{208}Pb/^{204}Pb$) can be used as a provenance tool. Given that Pb isotopes do not fractionate in low-temperature systems, groundwater Pb isotope ratios closely match those of the original source of Pb, be it the host-rock, mineralisation, or anthropogenic contamination (e.g. Caritat et al., 2005, Leybourne et al., 2009).

Geochemical indices combine pathfinder elements for a mineral system. An index (or ratio) enhances the sensitivity and reduces the variance of mineralisation anomalies in groundwater, given that saturation, solubility and analysis controls on any one element can lead to false negatives (and positives). Geochemical indices have been developed for direct groundwater mineral exploration (e.g. AuMin, NiMin) and for discriminating subsurface lithological changes relevant for the studied mineral system (e.g. Lithol1, FeS and AcidS; Gray et al., 2014, Gray et al., 2018). For example, Gray et al. (2014) developed the index AuMin (Au + Ag + As), which delineated major known gold camps in the northeast Yilgarn and flagged new anomalies in areas without known mineralisation. Although consideration of the local hydrogeological system and mineral system is required, these indices can be taken to other geological provinces as an exploration tool. Reid et al. (2021) found new subsurface anomalies using AuMin on groundwater in the Cobar region, New South Wales. However, prior to the present study, no attempt has been made to characterise the key hydrogeochemical features and build a geochemical index for sediment-hosted phosphate exploration.

Due to the complexity of groundwater systems, it has become common practice to conduct exploratory data analysis (EDA) on groundwater chemistry. EDA helps us understand the data and the influence of major hydrogeological processes (Grunsky, 2010; Zuo et al., 2021), with several approaches and diagrams standardised for water chemistry specifically (Güler et al., 2002). This is followed by applying more targeted multivariate statistical tools that reduce the data dimensionality, such as principal components analysis (PCA) and clustering, to unpack these underlying processes or characterise geochemical groupings of samples (Grunsky and Caritat, 2020; Güler et al., 2002; Zuo et al., 2021). To appropriately use these tools, it is important to use geochemical data in a non-compositional space, and thus it is standard to log-transform (clr, ilr or alr) them into Euclidean space (Buccianti and Grunsky, 2014; Egozcue et al., 2024). Multivariate approaches have been applied to transformed regional hydrogeochemical data to investigate and demonstrate hydrogeological processes including salinisation, recharge, mixing, WRIs, ion exchange and contamination (e.g. Cloutier et al., 2008; O'Shea and Jankowski, 2006; Walter et al., 2017; Zhang et al., 2014). When trace elements are included in the multivariate approaches, localised anomalies in pathfinder elements can be discovered and investigated. Gallagher et al. (2022) applied PCA and hierarchical cluster analysis to stream chemistry data and demonstrated that some of the anomalies in Cd and Zn were distinct from elevated metals sourced from peatlands and likely related to nearby mineralisation.

To this end, using the Northern Australia Hydrogeochemical Survey (NAHS; Schroder et al., 2020)—which is a comprehensive hydrogeochemistry dataset with a full suite of major, minor and trace elements and isotopes—we apply a combination of EDA and multivariate approaches in the Georgina Basin to determine:

1. the heterogeneity in the groundwater data and underlying hydrogeological processes;
2. if phosphate and/or Zn–Pb mineralisation is detectable in groundwater, and what spatial scale and sensitivity can be resolved; and
3. how robust the observed hydrogeochemical mineralisation relationships are and their suitability for other geological provinces and datasets.

2. Geological and hydrogeological setting

The Georgina Basin is an extensive intracratonic basin in the Northern Territory and western Queensland, with sediment packages from Cryogenian to Devonian age (Fig. 1). The northern half of the Georgina Basin (and lateral counterparts in the neighbouring Wiso Basin) is the focus of this work, which is comprised of mostly Cambrian limestones and siliciclastic sediments associated with shelf marine transgressions. This part of the Georgina Basin is subdivided into a series of Sub-basins (Beetaloo, Barkly, Central Georgina, and Undilla) and the NE-SW trending Alexandria-Wonarah Basement High, a paleo-ridge capped by Cambrian Kalkarindji Suite basalts that underlie much of the basin (Dixon-Jain et al., 2024; Kruse et al., 2013).

The dominant stratigraphic units in this region (Fig. S1) are the Gum Ridge Formation (and lateral equivalents such as the Thorntonia Limestone, Top Springs Limestone and Montejinni Limestone), conformably overlain by Anthony Lagoon Formation (and lateral equivalents such as the Wonarah Formation and Beetle Creek Formation). The Gum Ridge Formation is a variably dolomitic arenaceous limestone whereas the Anthony Lagoon Formation is a more siliciclastic package with interbeds of siltstone, sandstone and arenaceous limestone. Additionally, in the Central Georgina and Undilla Sub-basins, the Camooweal Dolostone (and V-Creek Limestone) are a late-stage Cambrian package of dolomitic carbonates that conformably overly the Anthony Lagoon Formation (Dixon-Jain et al., 2024; Dunster et al., 2007; Kruse et al., 2013).

These units make up the regional hydrostratigraphic Cambrian

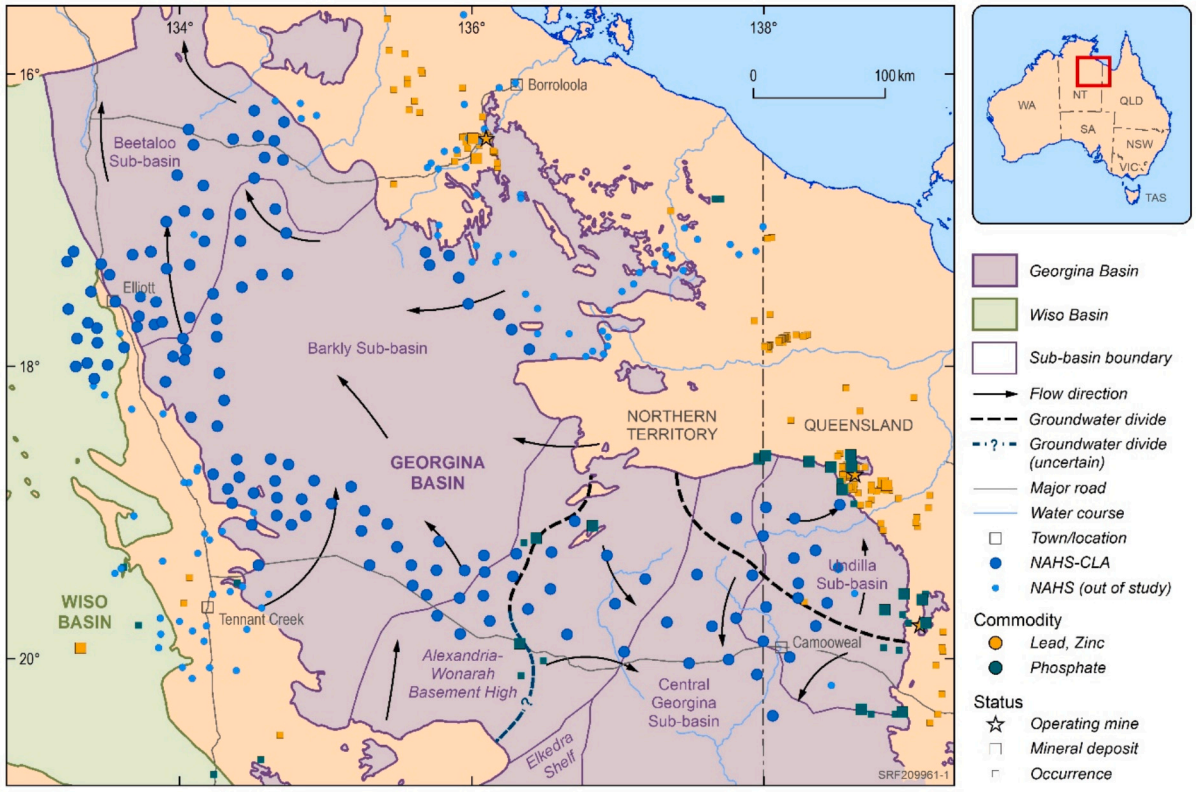

Fig. 1. Map of the central and northern Georgina Basin (and eastern Wiso Basin), showing the location of the Northern Australia Hydrogeochemical Survey (NAHS; Schroder et al., 2020) groundwater samples inside and outside the Cambrian Limestone Aquifer (CLA). Also shown is the distribution of phosphate and Zn–Pb mineralisation in and around the Georgina Basin (Geoscience Australia, 2020), and the generalised groundwater flow regime for the CLA (Dixon-Jain et al., 2024).

Limestone Aquifer (CLA), of which a representative cross-section is shown in Fig. 2. The CLA has high lateral connectivity via fractures and secondary karstic porosity. Vertical connectivity varies across the basin, but broadly there is a degree of inter-aquifer connectivity between the Gum Ridge and Anthony Lagoon formations. Siltstones of the Anthony Lagoon Formation act as local confining layers that can compartmentalise groundwater within the CLA (ELA, 2022). Groundwater recharge in the northern half of the Georgina Basin is predominantly via direct infiltration of rainfall and standing surface water following seasonal monsoonal events, where CLA units crop out on the basin margins (Dixon-Jain et al., 2024). A second recharge pathway involves infiltration of fresh precipitation via local sinkholes (where confining Cenozoic cover is absent) and mixing with much older groundwater (Deslandes et al., 2019). At a regional scale, the groundwater follows three main flow paths (Fig. 1). The Alexandria-Wonarah Basement High acts as a groundwater flow divide from which the Barkly Sub-basin groundwaters flow northwest to discharge into the Daly Basin and eventually the Roper River. East of this flow divide, groundwater from the Central Georgina Sub-basin flows south, while in the Undilla Sub-basin groundwater predominantly drains north into the Nicholson-Leichardt catchment (Dixon-Jain et al., 2024).

As well as hosting a significant groundwater resource, the Cambrian sediments of the CLA also contain multiple styles of mineralisation including sedimentary phosphate, sediment-hosted Zn–Pb, and stratiform Cu. In particular, the Georgina Basin accounts for over 95 % of Australia's demonstrated, economic phosphate resources (Dunster and Munson, 2017). The prevailing mineral system model for sedimentary phosphate requires upwelling of cold, organic and phosphate-rich waters onto shallow shelf environments or epeiric seas, often during high stands where terrestrial sediment supply is minimised. Phosphate is then deposited as *syn*-sedimentary francolite ($Ca_5(PO_4)_3F$) peloids or nodules via redox, physicochemical and microbial precipitation mechanisms. These phosphates can then be enriched into phosphorites (phosphate rich sedimentary rock) through biological reworking or diagenetic fluids mobilising P into redox fronts (Hill et al., 2024; Pufahl and Groat, 2017). According to this model, the margins of the Georgina Basin and the Alexandria-Wonarah Basement High would be the most prospective regions for phosphorites, which corresponds well to the distribution of known deposits (Dunster et al., 2007). These deposits are largely hosted in the Thorntonia Limestone and Beetle Creek Formation, with multiple studies investigating the phosphate's texture and geochemistry to understand the source of P, trapping and enrichment processes, as well as REE by-product potential (Creveling et al., 2014; Valetich et al., 2022; Zivak et al., 2024).

Sediment-hosted Zn–Pb deposits are more common along the Georgina Basin's southern margins (including the historic Box Hole mine), however, several occurrences have been found farther north in the Undilla Sub-basin (e.g. Tott's Creek; Dunster et al., 2007). Huston et al. (2019) reported the Pb isotope signature of sulfides from occurrences and mineralisation across the basin to be heterogenous, which is indicative of Mississippi Valley Type (MVT) mineralisation, as well as radiogenic, which is suggestive of 'Joplin-type' subgroup of MVT deposits (Dunster et al., 2007; Vaasjoki and Gulson, 1986). Beneficial characteristics for the formation and identification of a MVT mineral system are platform carbonates displaying brecciation or karstification creating voids for mineralisation as well as nearby faults providing pathways for low-temperature fluid flow and later stage dolomitisation (Wilkinson, 2013). These characteristics are frequently observed in Georgina Basin sequences, with the Thorntonia Limestone deemed one of the most prospective units for hosting MVT deposits (Cotter et al., 2002).

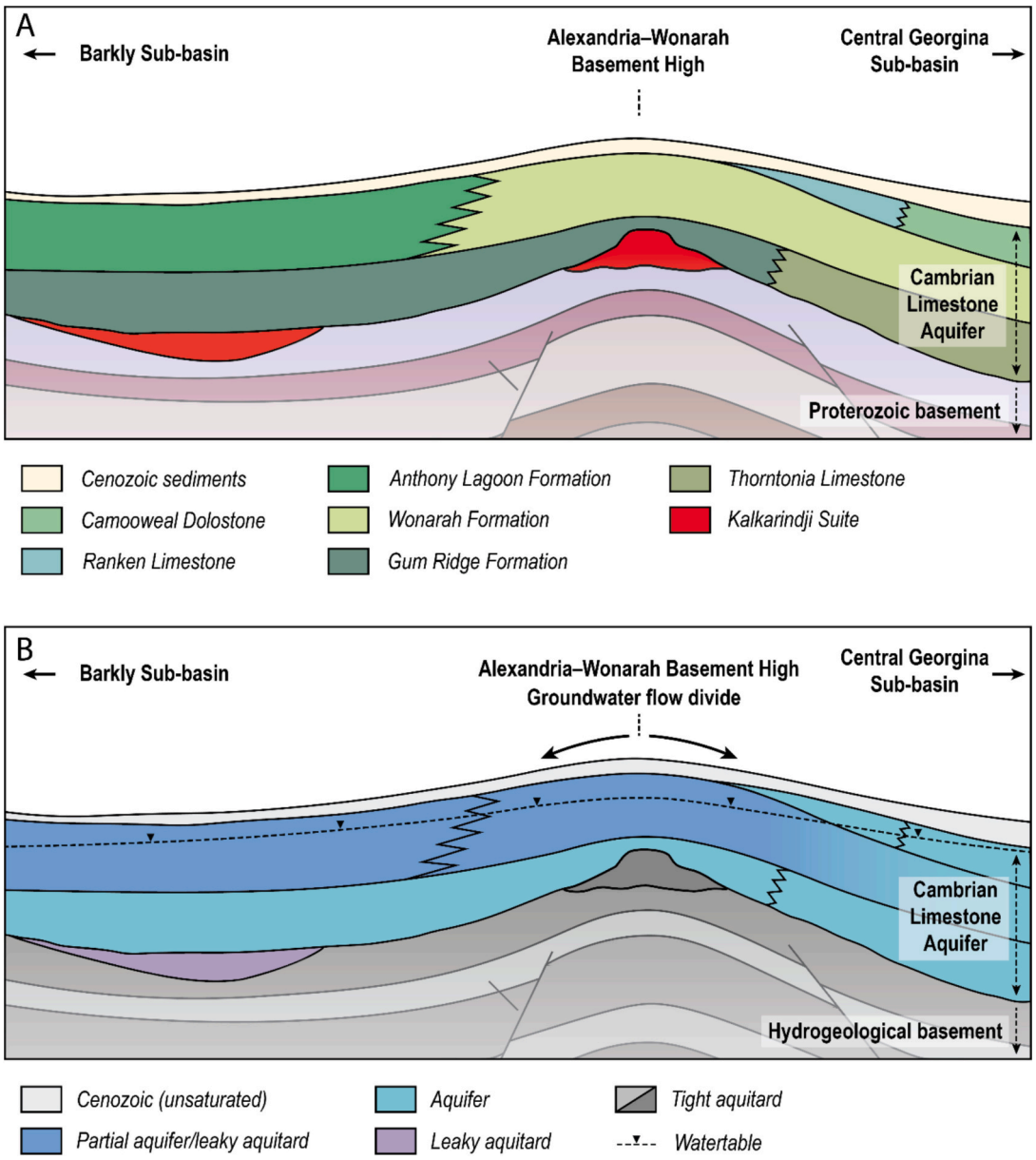

Fig. 2. A cross-section representation of the stratigraphy (2a) and hydrogeology (2b) of the Cambrian Limestone Aquifer (CLA), framed using a conceptual northwest-southeast transect across the Alexandria-Wonarah Basement High. Figure adapted from Dixon-Jain et al. (2024).

3. Methods

3.1. Groundwater sampling and data processing

Hydrogeochemical data in this study were sourced from the Northern Australia Hydrogeochemical Survey (NAHS; Schroder et al., 2020). Stringent sampling protocols were followed throughout the NAHS survey to prioritise sample integrity and ensure consistency and quality of the results. A brief overview is provided here but for more detail on the sampling and analytical methods, as well as the quality assurance processes, please refer to Schroder et al. (2020). Groundwater bores were pumped prior to sampling to remove stagnant water; arrival of fresh groundwater was assessed through monitoring for stable physicochemical parameters consistent with in-situ groundwater. Multiple bottles were collected at each bore, with different sampling methods depending on the requirements for different types of analysis. Broadly, samples requiring filtering were passed through a single-use, high-capacity 0.45 µm Waterra in-line filter capsule, and sample preservation was achieved either by acidifying with ultrapure 69 % HNO_3^-, or by filling the bottle completely (with no airgap) and refrigerated. All sample containers were rinsed three times with the water to be sampled. Field duplicates and laboratory duplicates were collected approximately every 10 samples to capture sampling and analytical uncertainty. Additionally, field and filter blanks were collected at the end of each field trip using Milli-Q® deionised water to capture systematic sampling and analytical bias.

Redox sensitive analytes (dissolved S^{2-} and Fe^{2+}) were measured in the field using a spectrophotometer. Total alkalinity was also measured in duplicate in the field via titration using a methyl orange indicator and reported as HCO_3^- (mg/L). Generally, analytical methods and instruments were selected to adhere to best practice and established methods for groundwater sampling (i.e. anions by ion chromatography, cations by ICP-OES, trace elements by ICP-MS), with a complete outline of the analytical methods and instruments for each field trip captured in Schroder et al. (2020).

Phosphorus concentration was reported both by ion chromatography (as PO_4^{3-}) and ICP-MS (as P). However, the ion chromatography results

were deemed unreliable due to the extended timespan between sampling and analysis coupled with the lack of sample stabilisation. Thus, all hydrogeochemical 'phosphate' results presented here refer to measurements converted from ICP-MS P. Additionally, a systematic positive bias (average 119.6 %) in Mg concentration for a subset of samples (sampleIDs s194-s281) was observed during review of analytical standards and batch duplicates. Mg values for the affected samples were reduced by the average bias (Schroder et al., 2020).

Within the NAHS dataset, the 35 Lake Woods groundwater samples were analysed for a slightly smaller subset of hydrochemical parameters, as summarised in Caritat et al. (2019). In total, this study assessed 238 groundwater bores sampled for a comprehensive suite of analytes, including major, minor and trace elements, as well as many stable isotope systems ($\delta^{18}O$ and $\delta^{2}H$ of water; $\delta^{13}C$ of dissolved inorganic carbon; $\delta^{34}S$ and $\delta^{18}O$ of dissolved sulfate; $^{87}Sr/^{86}Sr$ of dissolved strontium; and $^{206}Pb/^{204}Pb$, $^{207}Pb/^{204}Pb$ and $^{208}Pb/^{204}Pb$ of dissolved lead).

3.2. Hydrostratigraphic attribution and filtering

A manual hydrostratigraphic attribution process was conducted for each sample using a combination of local groundwater reports, drillers' logs, nearby stratigraphic holes (weighted for proximity), solid geology and surface geology. Given the focus on Georgina Basin (and equivalent) mineral systems, hydrostratigraphic attribution was necessary to ensure only samples within the CLA were retained for subsequent processing and analysis. Following this process, 143 NAHS samples were retained (hereafter referred to as NAHS-CLA).

This approach to hydrostratigraphic attribution is invariably subjective (our interpreted hydrostratigraphy and confidence is included in the Supplementary Dataset) and relied on both local hydrogeological knowledge and the proximity and quality of associated datasets. A moderately strict exclusion approach was taken for samples with some uncertainty regarding CLA hydrostratigraphy. Common sources for uncertainty included: wide screen intervals, local hydraulic connectivity suspected with the overlying Carpentaria Basin or Cenozoic paleovalleys; and deep, poorly logged samples on the basin margins. Despite best efforts, we expect some samples may have been retained that are not solely sourced from CLA aquifers or have local sources of contamination (i.e. recharge along the bore annulus). Thus, we have been cautious in reaching conclusions based on data patterns with fewer than seven samples (~5 % of NAHS-CLA).

3.3. Statistical analysis

In line with the methodology and principles of Grunsky (2010) for conducting EDA and multivariate statistics, NAHS-CLA data were further treated and transformed. A subset of elements was selected (Appendix 1) based on the criterion of having at least 70 % of concentrations above the detection limit (DL). This group was then imputed for null and censored values using the robCompositions library in R software following a two-stage process. First, null values were filled using impCODA with iterative trimmed least squares regression (Hron et al., 2010). The optimal k-nearest neighbour (knn) was determined by randomly removing 6 % of values and comparing the net accuracy of imputed versus the true value for knn 4–15, which was found to be knn = 6 for this dataset. Subsequently, censored (below DL) values were imputed using impRZilr with an iterative least squares regression (Templ et al., 2016) and the resultant dataset available in the Supplementary Material.

Initial investigations following imputation identified the need to exclude elements that displayed subtle analytical biases between surveys and/or had a spatial bias in pre-imputation elemental coverage (Fe, Ga, Ti, Co, Sc, Zr). With the exclusion of these elements, a smaller subset of geochemical species (Appendix 2) was then centre log-ratio (clr) transformed, followed by robust principal component analysis (rPCA) using low outlier rejection (Campbell, 1980). These principal components (PCs) were interpreted to provide insights into the dominant hydrogeochemical processes and element associations within the CLA.

Groundwater mineral saturation indices (SIs) were calculated in The Geochemist's Workbench® version 14 (Bethke et al., 2024), using the LLNL (thermo.tdat) thermodynamic database, with As, Fe, N and S species redox decoupled. SIs are a metric of how far a system is from equilibrium and are defined as the logarithm of the ratio of the (actual) ion activity product over the (thermodynamic) equilibrium constant; they are dimensionless (Bethke et al., 2024). Thermo.tdat was selected given it operates well for near-surface conditions (low-T, standard pressure), and has been found to more robustly evaluate phosphate mineral saturation (Sahai and Schoonen, 2020). Two samples (s176, s177) could not reach geochemical convergence and do not have SIs.

To ensure that changes observed in element concentrations relate to geochemical processes (such as WRIs) and not dilution or evapo(transpi)ration processes, elements were normalised to Total Dissolved Solids (TDS; mg/L) and are represented by an asterisk (*). The normalised ratios are thus dimensionless. To aid interpretation of these results, water-types of the NAHS-CLA were attributed using the quadrants of the Piper diagram (Piper, 1944) and are summarised in Fig. 3.

K-means cluster analysis was conducted in the ioGas™ software (v8.0). The input variables for clustering included all the elements used in rPCA (clr-transformed), electrical conductivity (EC, Box-Cox power-transformed), pH and Eh. All input variables were z-scaled. The optimal k (cluster count) from the elbow plot was deemed to be 6, from which some clusters were further sub-divided based on spatial groupings. Outliers were removed from clusters based on spatial isolation and/or sample-specific evidence for local hydrological deviation. Further details regarding the clustering method, results and outliers are documented in the Supplementary Material.

4. Results

4.1. Water composition

Summary statistics chemical composition of the NAHS-CLA samples are presented in the top half of Table 1. The full chemistry for all samples, as well as summary statistics for a larger subset of parameters, is included in the Supplementary Material. Previous studies of the hydrochemistry in this region (e.g. Caritat et al., 2019; Deslandes et al., 2019; Tickell and Bruwer, 2017) have shown that groundwater composition can be explained by the evolution of starting rainwater chemistry (Crosbie et al., 2012) which has experienced varying degrees of evapo(transpi)ration. From the starting rainfall compositions, many groundwater samples demonstrate relative enrichment in Ca, Mg and HCO_3^-, which is reflective of carbonate dissolution. The ratio of Ca to Mg remains relatively consistent across the region, driven by the prevalence of dolomite ($[Ca,Mg]CO_3$) in the CLA (Kruse et al., 2013). Additionally, a portion of the samples demonstrates relative enrichment of Na and K, which is likely due to incongruent dissolution of feldspars within the aquifer of recharge zone (Caritat et al., 2019). Several high-sulfate groundwater samples are observed (s14, s212, s217, LW014) which deviate considerably in composition from the other samples. These high-sulfate groundwaters lack any coherent spatial groupings, and given the associated high Ca in these samples, are likely capturing local dissolution of anhydrite ($CaSO_4$), a mineral that has been observed intermittently in drillholes across the basin (Kruse et al., 2013).

The Piper diagram (Piper, 1944) of Fig. 3b shows that a range of water compositions are hosted within the CLA. The distribution of these water-types is broadly consistent with interpreted hydrochemistry and hydrostratigraphy from Dixon-Jain et al. (2024) as well as the mapped distribution of the Gum Ridge Formation and Anthony Lagoon Formation in Tickell and Bruwer (2017). The Gum Ridge Formation and Montejinni Limestone (which are both dolomitic carbonate aquifers) are distributed on the margins of the basin and hold groundwaters of a

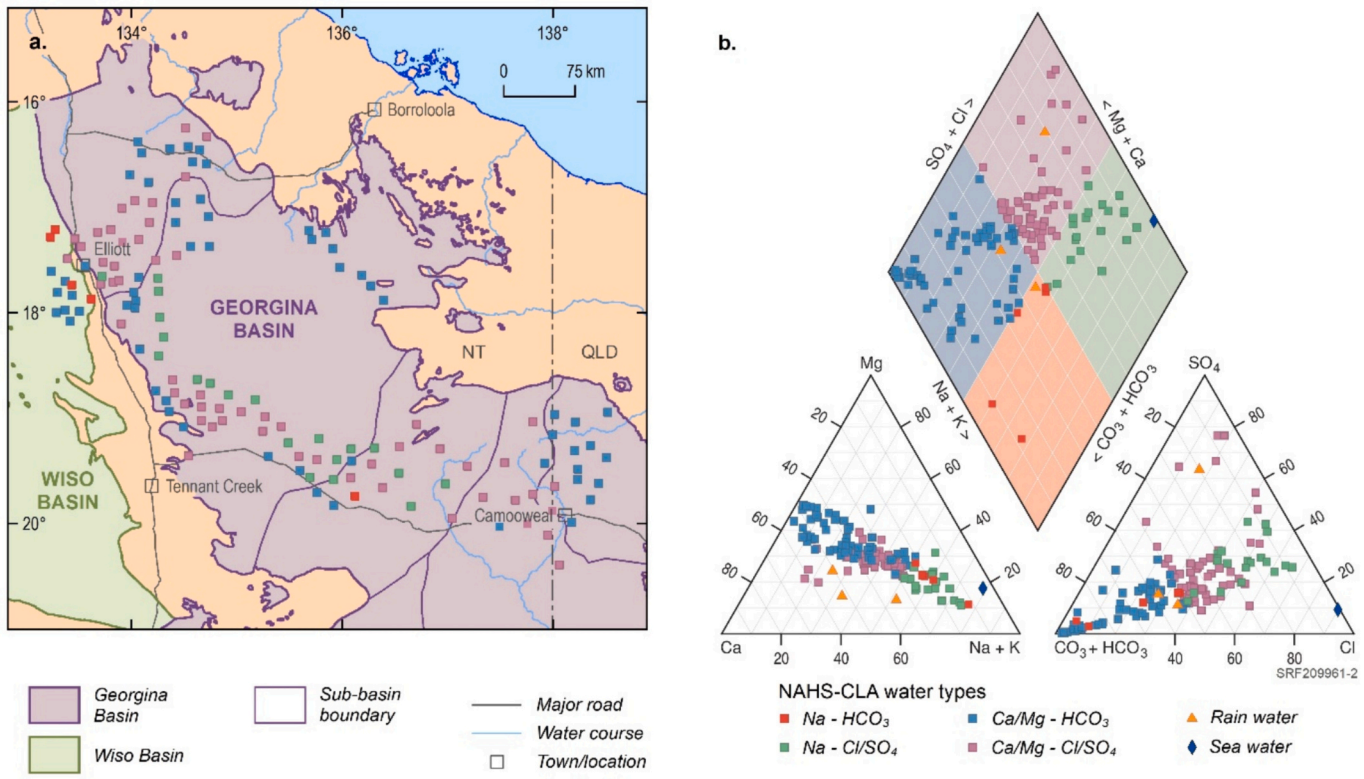

Fig. 3. a) Map of the NAHS-CLA samples coloured by water-type defined in Fig. 2b. b) Piper diagram (Piper, 1944) for these samples and the classification of each water-type. Average sea water composition is taken from Drever (1997), and rainwater compositions are from Crosbie et al. (2012), collected in Hall's Creek, Alice Springs and Mount Isa.

Ca-Mg-HCO_3^- composition. The Anthony Lagoon Formation (which is a more siliciclastic dominated aquifer), bears groundwaters of Na-Cl^--SO_4^{2-} and Ca-Mg-Cl^--SO_4^{2-} compositions. Groundwaters of the Na-Cl^--SO_4^{2-} water-type are more saline (mean TDS of 2341 mg/L compared with 1100 mg/L for the rest of the water-types) and are predominantly distributed in the centre of the Barkly Sub-basin. These Na-Cl^--SO_4^{2-} groundwaters are likely more strongly influenced by recharge via ephemeral lakes (e.g. Tarrabool Lake and Lake Sylvester; Tickell and Bruwer, 2017) which experience more significant evapo(transpi)ration than groundwaters recharging from the basin margins.

In the Central Georgina Sub-basin, the Ca-Mg-Cl^--SO_4^{2-} groundwater samples capture the eastward continuation of the Anthony Lagoon Formation (or equivalent Wonarah Formation). The transition to the karstic Camooweal Dolostone aquifer corresponds with a marked shift in groundwater chemistry to lower salinity, Ca-Mg-HCO_3^- groundwaters. This change in groundwater chemistry is attributed to the much higher carbonate content of the Camooweal Dolostone, and a shift to a landscape with much higher relief in the outcropping CLA (Dixon-Jain et al., 2024). Specifically, more rapid and localised groundwater recharge has been observed due to high permeability flow paths along the extensive karstic cave systems (Eberhard, 2003), which also reduces the influence of WRI and evapo(transpi)ration processes during infiltration of groundwater.

Very few Na-HCO_3^- groundwaters are observed in this region, and given the homogeneity of the CLA (at a high-level), each of these samples likely represents a different groundwater source and/or process from the rest of the dataset. The Na-HCO_3^- groundwater sample on the Alexandria-Wonarah Basement High is likely sourced from the basal Thorntonia Limestone, while the Na-HCO_3^- groundwaters observed in the Wiso Basin may represent groundwater sourced from the stratigraphically younger Point Wakefield beds.

4.2. Robust principal component analysis (rPCA)

Multivariate statistical tools such as rPCA are valuable for identifying geochemical and hydrogeological processes controlling the variance compositionally and spatially (Grunsky and Caritat, 2020). The goal was to test if groundwater interaction with CLA phosphate minerals is a significant geochemical process in this area, and if so, to develop a geochemical index (that doesn't solely rely on P concentration) as an indicator of phosphate prospectivity. Given the low solubility of Pb, too many groundwater samples were below the DL, which meant Pb could not be included in the rPCA to investigate spatial or element associations with Zn–Pb mineralisation. A full summary of the rPCA results is provided in the Supplementary Material.

Principal component 1 (PC1), which accounts for 28.6 % of the total variance, is capturing the salinisation of the groundwater (Fig. 4a), through evapo(transpi)ration, WRIs and cation exchange processes. Samples with more positive PC1 character are mostly less saline Ca-Mg-HCO_3^- groundwaters spatially distributed in the Wiso Basin, northeast Barkly Sub-basin and Undilla Sub-basin.

PC2, which accounts for 15.6 % of the geochemical variance, has weaker relationships, but is broadly capturing the basinward transit of groundwater from points of recharge (Fig. 4b-d). Samples with increasingly positive PC2 character tend to be older, more reduced and warmer, and occur in the Beetaloo Sub-basin and northeast Barkly Sub-basin. Samples with negative PC2 character conversely are generally younger, more oxidised and colder, and are found in the Wiso Basin and western flank of the Alexandria-Wonarah Basement High.

For the subsequent PCs, processes or groundwater relationships that affect the whole of NAHS-CLA could not be clearly identified. These PCs instead partially capture processes affecting a subset of samples. Of note is PC4, which accounts for 9.6 % of the total variance and is interpreted to be partly capturing potential P-mineralisation. Samples with more negative PC4 character are associated with elevated P, with spatial

Table 1
Summary statistics for the groundwater chemistry of NAHS-CLA samples, both as a complete dataset, and reported for the sub-groups defined after clustering. ^Mg reported using the corrected values as outlined in Section 4.1.

All data (143 samples)	TDS (mg/L)		Alkalinity as HCO_3^- (mg/L)		Ca (mg/L)		K (mg/L)		Mg (mg/L)^		Na (mg/L)		Cl^- (mg/L)		SO_4^{2-} (mg/L)		P (mg/L)
Mean	1273.5		438.3		119.3		21		67.5		160		224.06		206.77		0.0074
Median	1025.8		449.3		101.3		13.3		56		111.9		147.05		121.67		0.0052
SD	775.6		124.6		88.1		20		36.1		192.2		272.25		303.14		0.0072
Min	513.1		130.3		21.2		0.7		12.9		3.8		4.95		1.54		0.0001
Max	5008.2		744.1		675.9		122.3		217.5		1169.9		1830		1804.7		0.0542
Sub-groups	**Count**	**Mean**	**SD**	**Mean**	**SD**	**Mean**	**SD**	**Mean**	**SD**	**Mean**	**SD**	**Mean**	**SD**	**Mean**	**SD**	**Mean**	**SD**	**Mean**	**SD**
Cluster 1	14	1969.5	952.2	449.8	130.4	206.1	145.5	21.5	4.3	88.4	37.3	262.8	208.9	420.65	259.24	469.57	595.68	0.001	0.0012
Cluster 2a	11	764.5	113.1	502.5	73	92.1	24.7	6.4	1.9	46.3	5.5	25.7	31.6	25.72	26.89	31.72	43.25	0.0047	0.0047
Cluster 2b	10	822.4	103.8	571.3	83.4	93.9	14.7	1.9	0.9	68.7	11	18.5	16.3	28.47	35.26	15.61	19.86	0.0156	0.0044
Cluster 3	23	2203.3	1061.9	441	132.6	154.3	73.9	43.9	26.6	108.9	51.8	429.5	289.9	565.52	439.03	426.65	301.99	0.0072	0.004
Cluster 4	14	775.5	153.4	461.5	79.6	56.2	14.3	33.6	13.6	33.2	9.6	57.6	39.9	41.9	33.4	25.52	27.8	0.0093	0.0132
Cluster 5a	16	1135.1	220.1	432.7	123.1	87.1	21.7	22.3	15.4	52.3	7.9	143.7	47.9	216.87	49.83	141.63	47.45	0.0045	0.0039
Cluster 5b	8	1167.6	304.4	522.8	154.5	92	17.5	31.4	30.7	71.7	15.6	133.8	71.2	163.77	81.16	103.01	52.79	0.0091	0.0061
Cluster 5c	14	936.8	259.7	336.4	97.1	102.4	33.6	7	4.2	60	17.4	99.9	39.3	179.19	79.41	134.26	53.09	0.0118	0.0064
Cluster 6	24	1039.8	342.5	386.3	82	120.6	71.3	12.2	4.1	56	15.4	96.6	64.6	135.43	98.05	207.72	204.37	0.006	0.0072
Outlier	9	1200.3	789.5	383.8	158.6	158.9	197.4	15.1	14	73.1	47.4	106.5	90	161.29	160.71	262.68	480.83	0.0093	0.0061

grouping in the Central Georgina Sub-basin and Undilla Sub-basin. This relationship will be explored further in Section 5.3.1.

4.3. Elemental P relationships

As a starting point for investigating P in groundwater, we look at the mineral saturation of phosphate minerals, in this case hydroxyapatite's SI (Fig. 5) in the NAHS-CLA dataset. Two populations are immediately evident, with most samples saturated (SI ~ 0) or oversaturated (SI up to ~6) with respect to hydroxyapatite ($Ca_5(PO_4)_3(OH)$), while a smaller subset is significantly undersaturated (SI < 0). The undersaturated subset does not have any clear distinct geochemical or physicochemical differences from the rest of the samples. Spatially, a large cluster of these undersaturated samples is on the southwestern margin of the Barkly Sub-basin (Fig. 6), which, given that groundwater is recharging along this margin (Dixon-Jain et al., 2024), would suggest that no phosphate has been encountered along the flow-path. The remainder of the undersaturated samples are in the Wiso Basin and southern Barkly Sub-basin and are suspected to reflect local hydrogeological controls and stratigraphic changes for those samples which will be discussed more further on.

Caution is needed in relying too strongly in SIs for phosphate minerals, which have been found to have large differences between different thermodynamic databases (Oelkers et al., 2009). Sahai and Schoonen (2020) found that many thermodynamic databases overestimate hydroxyapatite solubility, and recommended using thermo.tdat which held up most consistently with empirical experiments. For this reason the SIs presented here were generated from thermo.tdat (Fig. 5), noting that the subset of samples identified as highly undersaturated in hydroxyapatite (SI ~ −29 to −38) still broadly have lower hydroxyapatite SIs using other thermodynamic databases (approximately −7 to −13 using thermo_phreeqc.tdat or thermo_wateq4f.tdat) so would not meaningfully change the interpretation.

Most of the samples are saturated or over-saturated with respect to P minerals (Fig. 5). This means P concentration by itself is not a reliable indicator of nearby mineralisation as there is limited capacity of the saturated groundwater to dissolve more P when in contact with phosphorites. Thus, an effective prospection tool would require identifying suitable indicator elements for phosphate mineralisation alongside P that do not reach saturation, do not have other common mineral sources, and ideally have similar redox behaviour to P in groundwater to ensure concomitant transport. Francolite (or carbonate-rich fluorapatite) is the most common primary sedimentary phosphate mineral. From a theoretical perspective, dissolution of francolite would yield an increase in Ca and F^- in the groundwater, and we would also expect to see associated increases in elements that commonly substitute in the francolite lattice such as Mg, Sr, Na, CO_3^{2-}, SO_4^{2-} and OH^- (Pufahl and Groat, 2017). However, with the exception of F^-, these species are common to many sedimentary minerals in the CLA, most notably in carbonates and feldspars, which confounds any correlations with P we might hope to see in the groundwater chemistry. Fluoride also is not a viable tracer for phosphates in this groundwater system, as it may precipitate as the very low solubility mineral fluorite (CaF_2) if any dissolved Ca exists in the groundwater. Common trace element substitutions in francolite include Se, Mo, Zn, Cu, Cr, U and REEs (Pan and Fleet, 2002; Pufahl and Groat, 2017). No P relationships were observed with these elements across the NAHS-CLA dataset, with low metal solubility and concentrations near (or below) DLs limiting the potential of many of these species as pathfinders for phosphorite.

Given this, we approached the question of predicting phosphate prospectivity from an empirical perspective, utilising the rPCA results where PC4 was interpreted to (in part) reflect groundwater interaction with phosphorites within the CLA. This interpretation is supported by the spatial association of negative PC4 samples with the eastern margins of the Georgina Basin (Fig. 6), which host most known phosphorite deposits. From the eigenvectors, the main elements correlated with P in

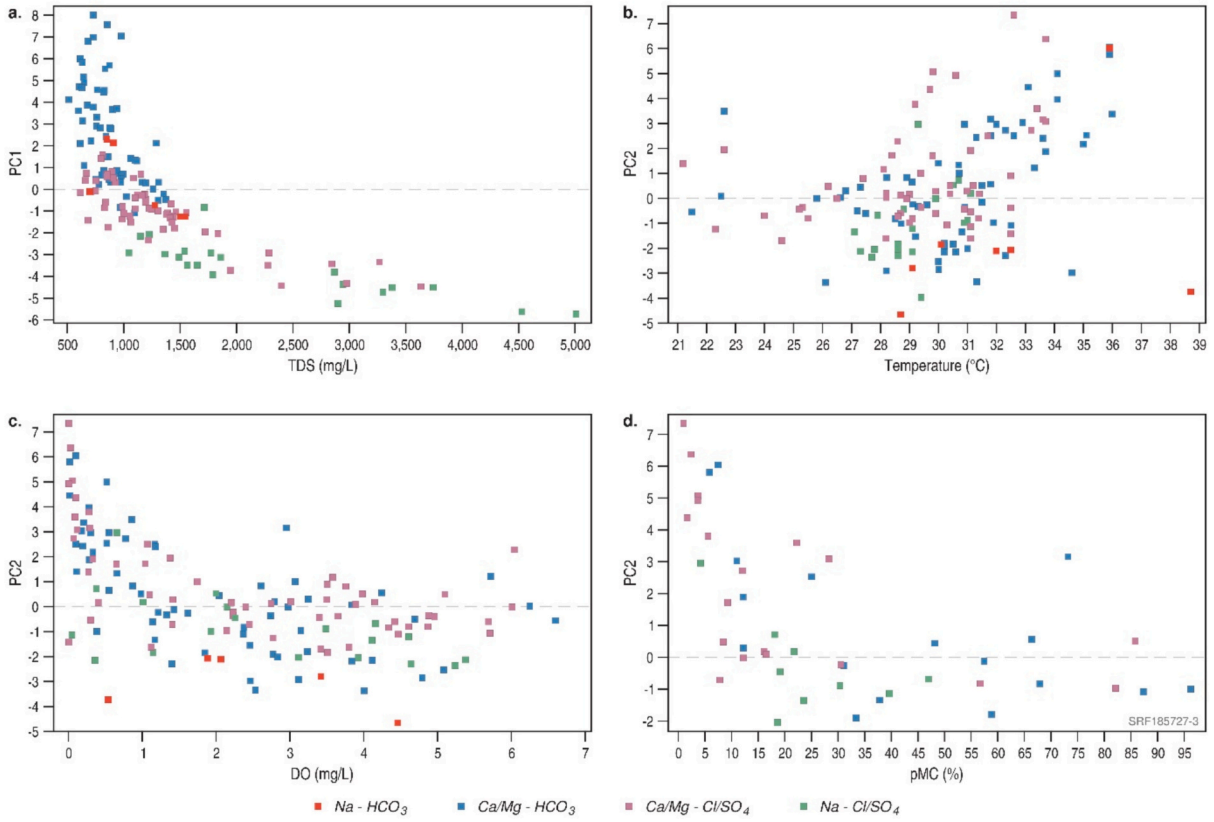

Fig. 4. NAHS-CLA samples following rPCA and coloured by water-type (see Fig. 3b). a) PC1 vs Total Dissolved Solids (TDS, in mg/L). b) PC2 vs Temperature (°C). c) PC2 vs Dissolved Oxygen (DO, in mg/L). d) PC2 vs percent modern carbon (pMC, in %).

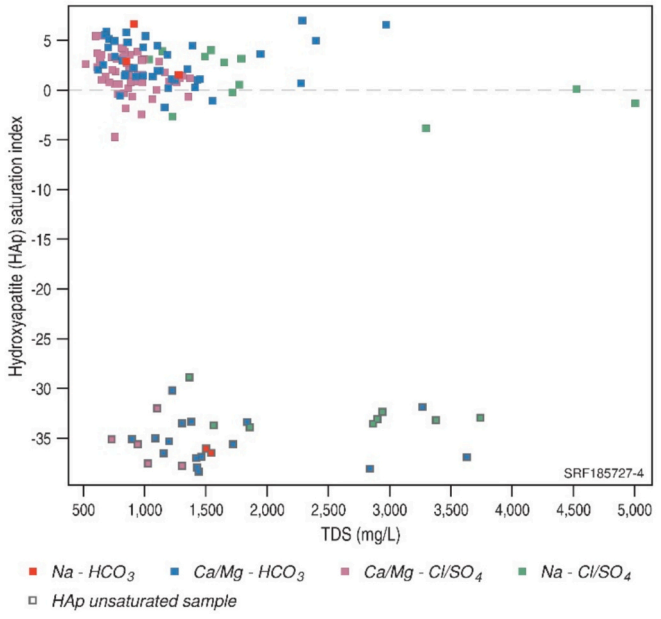

Fig. 5. The saturation index of hydroxyapatite (HAp) against Total Dissolved Solids (TDS, in mg/L) for the NAHS-CLA samples. Most samples are at saturation or oversaturated. Samples are coloured by major water-type (see Fig. 3b). Samples highly undersaturated are outlined with black which will be carried through to subsequent figures.

PC4 are Mo and Al, while I^- and Rb are inversely associated elements (Fig. 6). However, when considering the whole of the NAHS-CLA, no correlation is evident between P* and these elements. A more nuanced approach was needed to explore if there were robust relationships of P* (P normalised to TDS) in subgroups of the data. Multiple methods for grouping the data were considered and tested. Ideally, groups of data would be defined by hydrogeologically relevant features, such as groundwater regions (defined by flow divides) and/or aquifer compositions. However, for much of the CLA, the groundwater recharge, flow dynamics, and aquifer composition have only coarse regional constraints which are not robust enough to reliably subdivide the samples (Dixon-Jain et al., 2024).

4.3.1. *P relationships in clusters*

Cluster analysis is a data-driven tool for investigating subrelationships and partitioning within a dataset by evaluating the similarity between samples in multivariate space (Templ et al., 2008). Our primary goal of implementing k-means clustering was to independently subdivide the dataset, to investigate which clusters (if any) depict the PC4 element associations. The geochemistry within each cluster subgroup is summarised in the bottom half of Table 1. Following cluster analysis, three sub-groups were identified (clusters 2b, 3 and 5c) where P* holds a linear relationship with either Mo*, I*, Rb* and/or Al* (Fig. 7b and c and summarised in Table S1). Cluster 5c demonstrates the strongest correlation of P* with both Mo* ($R^2 = 0.72$) and I* ($R^2 = 0.58$), whereas clusters 2b and 3 have weaker relationships that appear to be affected by the presence of outliers. Only cluster 3 has any correlation between P* and Al*, thus suitability of Al as a supporting element for vectoring towards phosphate mineralisation is less reliable. Additionally, if the samples highly undersaturated in hydroxyapatite are considered a separate subgroup and removed from cluster 3, the relationships of P* with the other elements for cluster 3 become much stronger (R^2: Mo* = 0.37, I* = 0.24, Al* = 0.56). We further investigated if any elements that commonly occur or substitute in francolite (i.e. U, REEs, F^-, Mo) had relationships with P within these clusters, but with

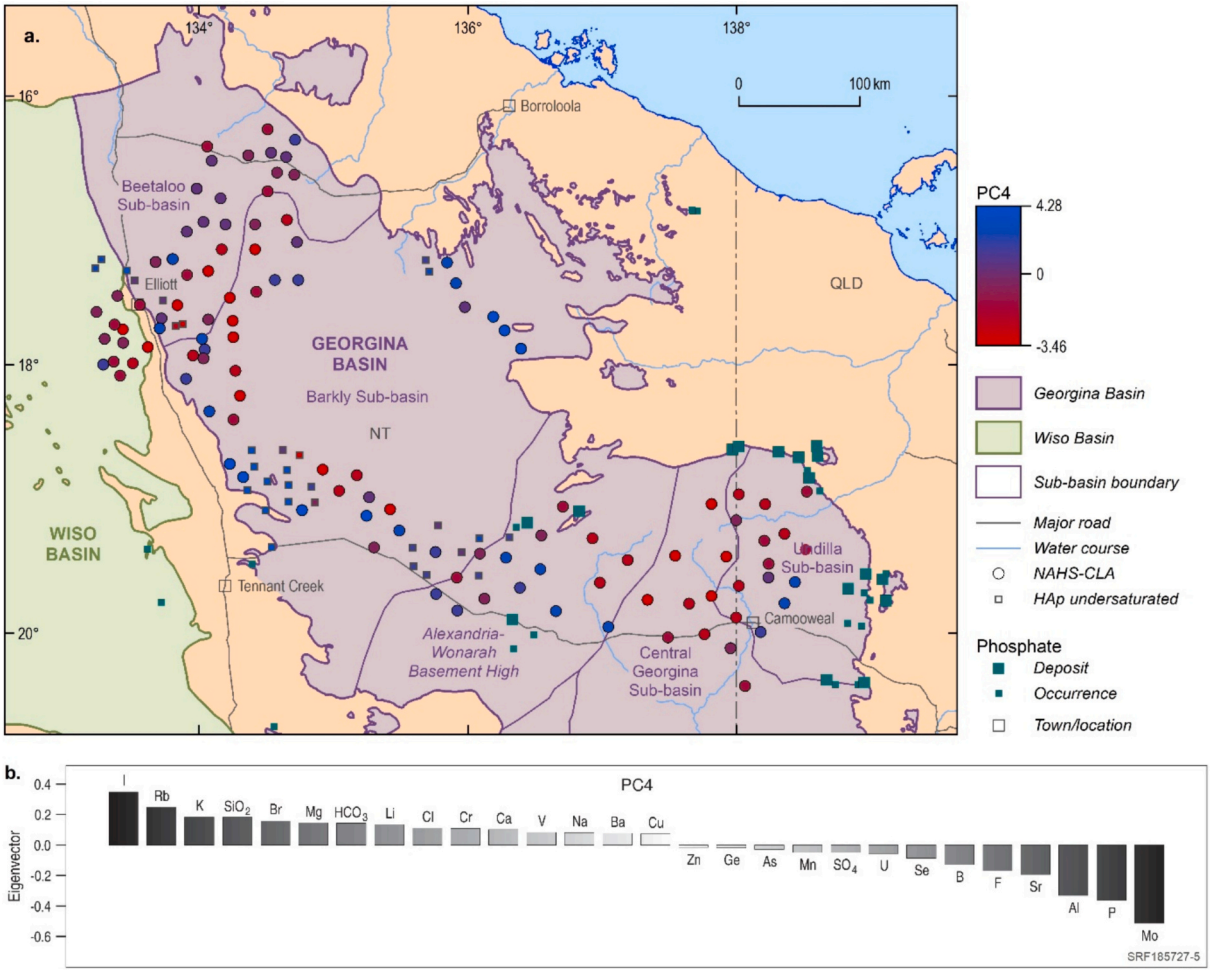

Fig. 6. The relationship of PC4 in NAHS CLA samples. a) Map of PC4 for NAHS-CLA samples and known phosphate mineralisation (Geoscience Australia, 2020), with NAHS-CLA points coloured based on their compositional relationships of elements in PC4. b) Ranked eigenvectors of PC4, showing the associations of the 28 species in this PC.

the exception of Mo, no relationships were observed.

Relating these clusters to known phosphorites, Cluster 2b is proximal to known phosphorite deposits on the Georgina Basin's eastern margin, while Cluster 3 is located downflow from both the Wonarah deposit and the high P_2O_5 intervals observed in Georgina Basin sediments from drill core on the Alexandria-Wonarah Basement High (Schroder et al., 2024a, b). The Central Georgina Sub-basin, which contains predominantly cluster 5c samples, has phosphorites distributed on its northwest and eastern margins, though this likely under-represents the occurrence of phosphorites in this region given the greater depth of the phosphate-bearing Thorntonia Limestone.

4.3.2. Phosphate geochemical index

The rPCA has identified the key geochemical associations of P in the NAHS-CLA, and clustering has helped refine which associations are most likely indicators of phosphate mineralisation. From this we can develop an overarching geochemical index for assessing phosphate prospectivity that hones in on targets for exploration, irrespective of clusters and water-types. P* is a clear indicator element for phosphate mineralisation. Further elements (Mo*, I*) were selected for the index based on their more consistent and stronger relationships with P* across the subgroups (2b, 3, 5c) spatially associated with known mineralisation. The geochemical rationale for the elements associated with P* and those chosen for *Phos#* are further discussed in Section 6.2. These elements are combined to define a geochemical index for phosphate prospectivity, *Phos#* (Eq. 1) (* indicates concentration normalised to TDS).

$$\mathrm{Phos}^{\#} = (\mathrm{P}^{*} \times \mathrm{Mo}^{*}/\mathrm{I}^{*}) \times 10^{6} \quad (1)$$

In *Phos#*, elements are normalised to TDS to reduce the influence of evaporative enrichment and mixing dilution on the concentrations; *Phos#'s* constituents are dimensionless, so it too is dimensionless. Normalisation does make the results of the equation very small, so it is multiplied by 10^6 for ease of viewing and interpretation. Outliers in the *Phos#* index are identified from Tukey's upper outlier (or inner fence) threshold (Tukey, 1977) and are inferred to represent WRIs of groundwater with local phosphate mineralisation (Fig. 8). Groupings of *Phos#* outliers combined with local hydrogeological knowledge (i.e. groundwater flow direction, vertical mixing) could then be used to vector towards mineralisation. In Fig. 8, as well as expected outliers in the Undilla Sub-basin (ellipse 1), this approach raises several prospective regions for further phosphate exploration: the Central Georgina Sub-basin (ellipse 2), the boundary between the Beetaloo Sub-basin and Barkly Sub-basin (ellipse 3) and on the east and west flanks of the Tomkinson Province (ellipses 4 and 5).

4.4. Sediment-hosted Zn–Pb

Trace element hydrogeochemistry from the NAHS-CLA can also be used as a first pass tool for identifying anomalies indicative of sediment-hosted Zn–Pb mineralisation. Fig. 9 shows Pb* and Zn*, with upper outliers symbolised (defined via Tukey boxplots in Fig. S5; Tukey, 1977). Spatially, the outliers are relatively spread-out with outlier

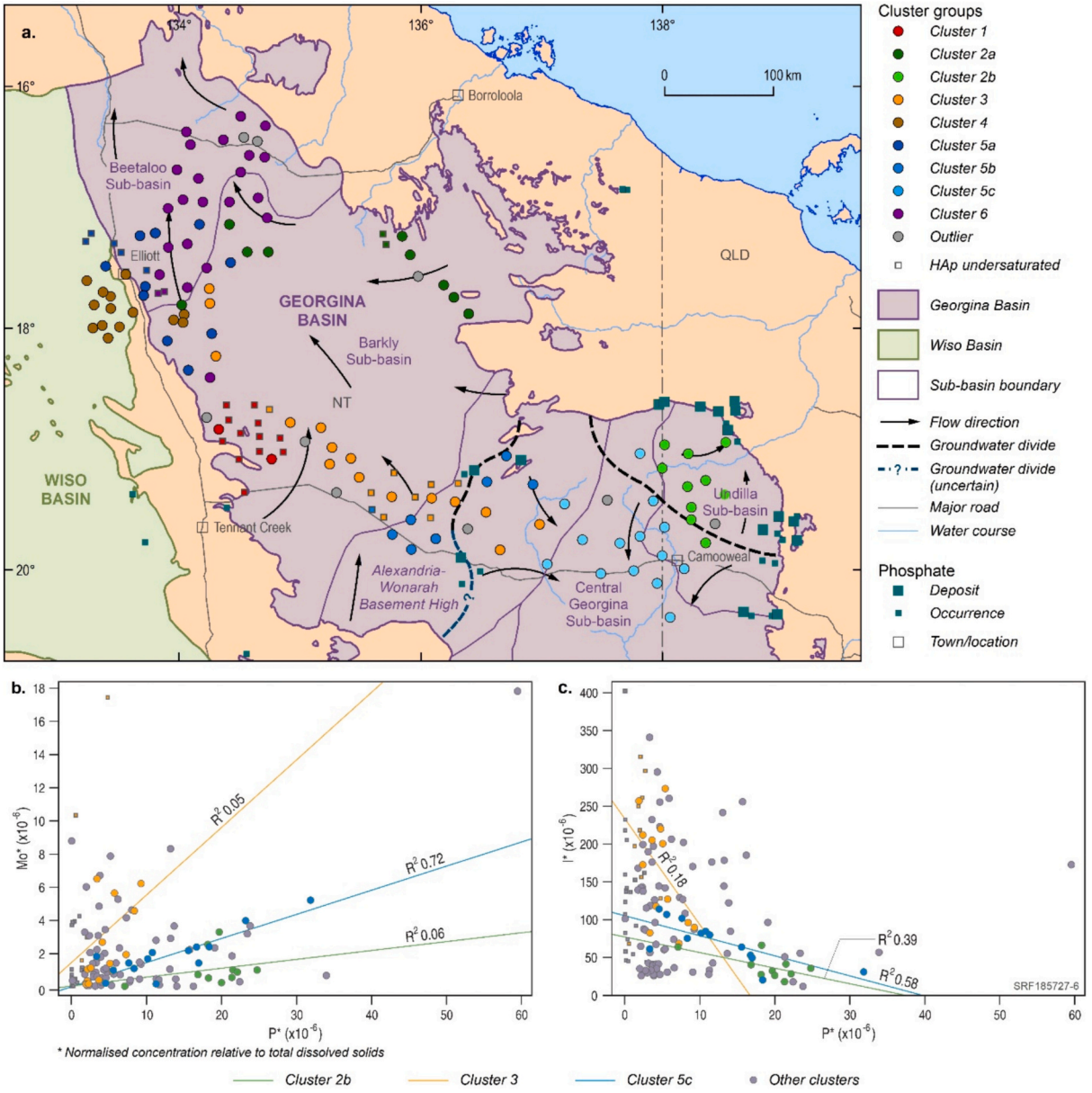

Fig. 7. The NAHS-CLA dataset classified by k-means clustering and interpretation. Samples highly undersaturated in hydroxyapatite (HAp; see Fig. 5) are shown as smaller squares. a) A map of the groundwater clusters and outliers with known phosphate mineralisation (Geoscience Australia, 2020). Arrows and dashed lines indicate groundwater flow direction and groundwater flow divides, respectively, taken from Dixon-Jain et al. (2024). b;c) Plots of Mo* and I* against P* (dimensionless), where * represents concentration normalised to total dissolved solids (TDS). Clusters 2b, 3 and 5c retain their colour from Fig. 6a as clusters with observed P relationships, with remaining samples grouped in gray. The linear regressions are further described in Table S1 of the Supplementary Material.

clusters only occurring in the Central Georgina Sub-basin, Undilla Sub-basin and western Beetaloo Sub-basin, and rarely for both metals concurrently. These concentration results must be interpreted with caution, however, as the NAHS-CLA's sample density (~1 per 400 km^2) is much sparser than the expected size of a metal-enriched groundwater plume coming off a deposit (depending on the element and groundwater conditions, Caritat and Kirste (2005a, b) modelled metal-enriched plumes of between 100 and 3000 m). This means a plume would only be intersected by 1–2 samples (if at all), although if mineralisation is extensive, multiple plumes may be present and detectable via groundwater across a larger area. Additionally, the low solubility of Pb (and to a lesser extent Zn) limits any increase in dissolved metals and requires comparing concentrations near the analytical DL, which hold greater analytical uncertainty (Champion et al., 2020). Hydrogeochemical anomalies observed in only a few samples are a high risk of being false positives, whether because of sampling or analytical uncertainty (Grunsky and Caritat, 2020; Leybourne and Cameron, 2010), being sourced from a different aquifer, or locally different hydrogeological conditions (unrelated to mineralisation).

More confidence in the validity of these metal concentration anomalies can be gained by integrating with related isotope system(s), which can provide independent insight into the metal's source (lithology or mineralisation), and geochemical weathering processes (Caritat et al., 2005, Kidder et al., 2021, Mahan et al., 2023). Previous work by Leybourne et al. (2009) demonstrated that Pb isotopes in groundwater are sensitive enough to differentiate sources of Pb, even if Pb concentrations are below conventional analytical detection limits. The Pb isotope ratios for the NAHS-CLA (of which $^{206}Pb/^{204}Pb$ is plotted in Fig. 9, as well as Figs. S6 and S7) display a significant range of compositions that follow well-defined arrays ($^{206}Pb/^{204}Pb$: 16.459–22.671, $^{207}Pb/^{204}Pb$: 15.528–16.231, $^{208}Pb/^{204}Pb$: 36.294–42.533). Potential sources of the Pb include rock units of the CLA, rock units underlying the CLA (i.e. the Kalkarindji Suite or

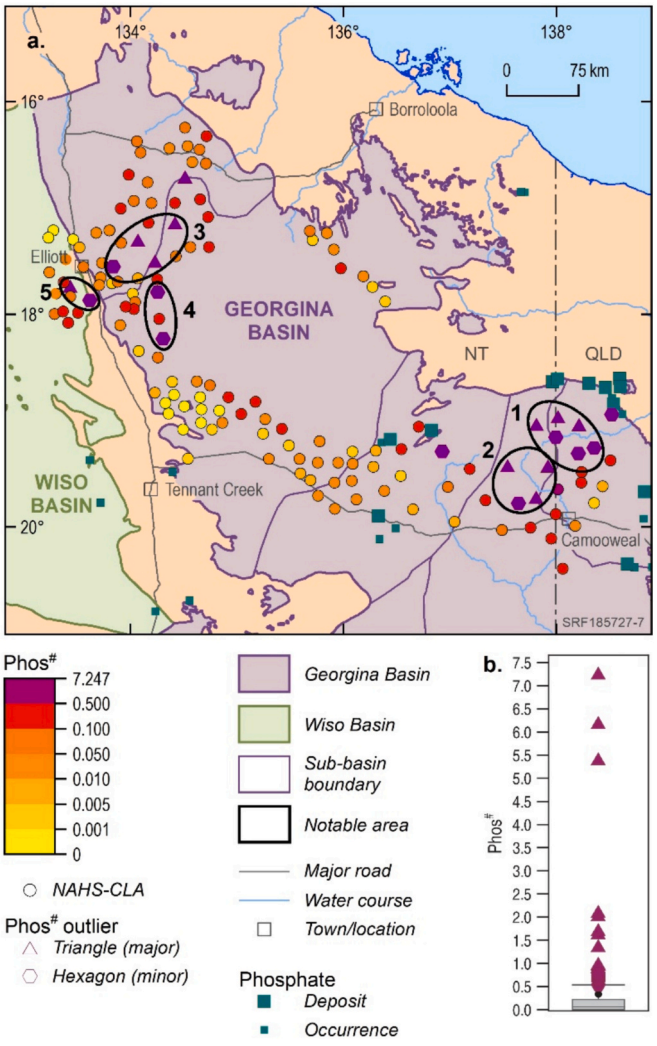

Fig. 8. a) Map of the derived geochemical index *Phos#* (Eq. 1) for NAHS samples in the CLA (coloured circles) with known phosphate mineralisation (green squares; Geoscience Australia, 2020). Samples exceeding Tukey's upper outlier thresholds (from Fig. 8b) are plotted as larger purple hexagons and triangles. Areas with spatially adjacent outliers (black ellipses) have been identified as the most prospective regions to follow up. b) Tukey boxplot (Tukey, 1977) for *Phos#* for NAHS-CLA samples with outliers and extreme outliers symbolised (as hexagons and triangles, respectively). (For interpretation of the references to colour in this figure legend, the reader is referred to the web version of this article.)

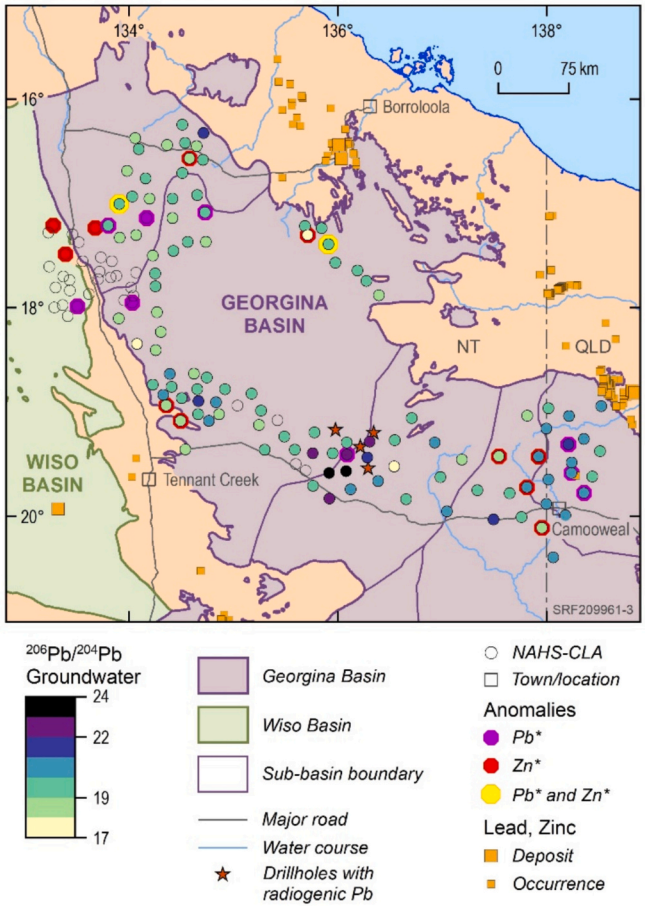

Fig. 9. Map of $^{206}Pb/^{204}Pb$ for NAHS-CLA with known Zn–Pb mineralisation (Geoscience Australia, 2020). Higher ratios are interpreted to be sourced from WRI or weathering of host rocks containing a 'Joplin-type' MVT Pb isotope signature (Huston and Champion, 2023). Outlined samples have upper (Tukey) outlier concentrations of Zn* and/or Pb* (concentrations normalised by TDS). Recently analysed drillholes containing whole-rock samples with radiogenic Pb signature are mapped (Schroder et al., 2024b) to contextualise the groundwater Pb isotope anomalies observed across the Alexandria-Wonarah Basement High.

Proterozoic basement), and Pb-rich mineralisation in the basin (or basement).

Although a reasonable amount of Pb isotope data exists for mineral deposits and occurrences in this region (Huston et al., 2019 and references therein), the Pb isotope signatures for background lithology of the basin and basement are limited. We can rule out the underlying Kalkarindji Suite basalts have a strong influence on the groundwater, given the distinctly different Pb isotope signature (Fig. S7) of these mafic rocks (Ware et al., 2018). However, for other potential Pb sources, the lack of Pb isotope coverage makes it challenging to assess what constitutes a significant deviation from the background Pb isotope signature that would be indicative of mineralisation (or other hydrogeological changes). Despite these limitations, we still identify promising indications of mineralisation from the Pb isotopes in the groundwater. Particularly where the upper and lower tails in the distribution of NAHS-CLA Pb isotope values align with the known end-member compositions for mineralisation in the Georgina Basin and basement respectively. In several examples (discussed more below), these similarities in Pb isotope values between groundwater and mineralisation are validated by spatial proximity to small-scale mineralisation.

The less radiogenic groundwater values in the NAHS-CLA (but observed more frequently in the larger NAHS dataset; Figs. S6 and S7) trend towards Pb isotope signatures of ore deposits and occurrences hosted in Proterozoic basement (Huston et al., 2019). Several of the least radiogenic samples (i.e. s84, s185) are observed on the flanks of the McArthur Basin and Tomkinson Province respectively, which we interpret to reflect the influence of basement, including possible mineralised rock.

Conversely, the most radiogenic values in the NAHS-CLA trend towards the Pb isotope signature of Georgina Basin's 'Joplin-type' MVT Zn–Pb mineralisation, which is highly radiogenic ($^{206}Pb/^{204}Pb$: 19.497–30.025; Huston et al., 2019, Schroder et al., 2024b) and quite heterogeneous (as is typical of MVT deposits; Wilkinson, 2013). When overlaid with trace element anomalies of Pb* or Zn* (Fig. 9), the high values in the Undilla Sub-basin are supported by one nearby radiogenic Pb isotope sample located very near to outcropping Zn–Pb mineralisation at Tott's Creek (Dunster et al., 2007). The remaining Pb* or Zn* outliers are not corroborated by Pb isotope outliers; however, several further areas of interest are captured solely in the Pb isotopes. In Fig. 9, we observe a highly radiogenic Pb isotope anomaly comprising multiple

samples ($^{206}Pb/^{204}Pb$ of 22–24) situated on the Alexandria-Wonarah Basement High. These radiogenic groundwaters align spatially and hydrostratigraphically with whole-rock Pb isotopes collected from Pb-rich, sulfide-bearing CLA rocks ($^{206}Pb/^{204}Pb$ of 22.5–23.0; Schroder et al., 2024b), supporting the assertion that radiogenic Pb isotopes in the NAHS-CLA reflect a mineralisation signature. One sample in the north-eastern Beetaloo Sub-basin also has a radiogenic Pb isotope signature. No known Zn–Pb mineralisation exists in this part of the Georgina Basin, however, logs from a nearby drillhole (Tanumbirini 1) have noted pyrite nodules and Fe-mineralisation within the Gum Ridge Formation, which is suggestive of some later stage redox sensitive fluid.

5. Discussion

5.1. Primary vs secondary phosphate mineralisation

Further insights can be gleaned regarding hydrogeochemical anomalies with a thorough understanding of the local mineral system. New downhole whole-rock geochemistry and portable X-ray fluorescence profiles from nine drillholes on the Alexandria-Wonarah Basement High have revealed three distinct zones of P_2O_5 (and base metal) enrichment in the Georgina Basin sediments (Schroder et al., 2024b):

(1) A 'supergene' zone, from approximately 10 to 30 m depth below surface, comprising variably weathered, in-situ Georgina Basin sediments;

(2) a 'water intercept' zone from approximately 40 to 75 m depth, correlating with the first (major) water intercept below surface (identified from bore reports); and,

(3) primary phosphate mineralisation in the unweathered, basal Cambrian sediments of the Thorntonia Limestone.

The 'supergene' and 'water intercept' zones are interpreted as secondary phosphate mineralisation, derived from weathering and meteoric transport of commodity elements from deeper primary mineralisation in the basin (Fig. 10). The transported P (and metals) are deposited or adsorbed at the redox interfaces associated with groundwater boundaries at these shallower depths over long timescales, often alongside metal-(oxyhydr)oxides and clays (Creveling et al., 2014, Schroder et al., 2024b).

Interpreting the *Phos#* results in the context of the redox zones introduced by Schroder et al. (2024b), as well as our knowledge of the hydrogeology and groundwater flow pathways, gives further insights into the source and prospectivity of the *Phos#* ellipses (Fig. 8). Ellipse 1 outliers are likely derived from either secondary phosphate sourced from weathering of phosphorites to the north and east, or undiscovered phosphorites straddling the groundwater flow divide between the Undilla and Central-Georgina Sub-basins (see Fig. 7a for the flow divides). The mechanisms for forming and preserving these secondary phosphate intervals are discussed further in Schroder et al. (2024b). The same weathering processes are thought to explain the outlier cluster in ellipse 2. However, developing secondary phosphate enrichment here away from the Georgina Basin's margins likely requires a source of primary phosphorites distinct from those on the eastern margin. These are suspected to be from proximal deeper primary phosphorites in the Thorntonia Limestone and on the Alexandria-Wonarah Basement High. Importantly, ellipse 1 and 2 outliers are detecting secondary phosphorites, this can still be a significant mineral resource, as demonstrated by the Wonarah deposit, which exhibits secondary supergene mineralisation within the Gum Ridge Formation (Lilley and Broadbent, 2002). Ellipses 3, 4 and 5 do not align with any known phosphorites (primary or secondary), and highlight areas of greenfield interest for future phosphate exploration in the Georgina Basin and Wiso Basin.

Further validation of this redox-controlled, geochemical enrichment model would best be done by targeted sampling of these interfaces across the basin. Analysis of whole rock and mineral (i.e. clays, phosphates and metal-(oxyhydr)oxides) chemistry would support understanding of the geochemical patterns at a more local scale as well as the controls on the deportment of both P and indicator elements. Additionally, testing the prospectivity of *Phos#* would likely require new drilling up-flow of the regions within the ellipses, seeking to intersect both the 'water intercept' zone and the base of the CLA to ascertain primary versus secondary mineralisation.

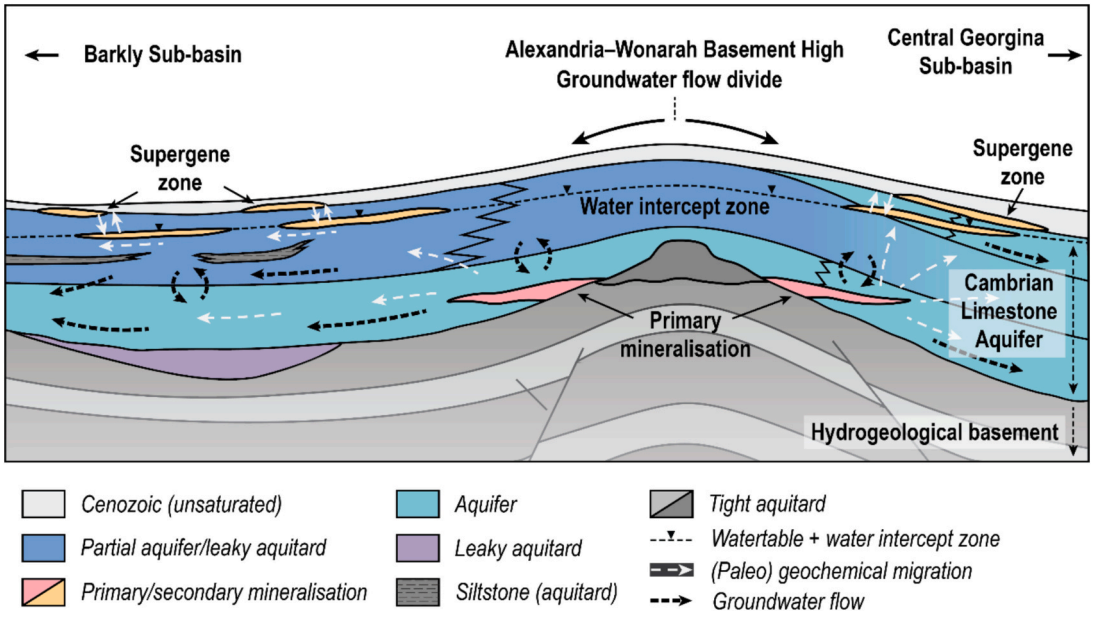

Fig. 10. A cross-section representation of the hydrogeology of the Cambrian Limestone Aquifer (CLA), framed using a conceptual NW-SE transect across the Alexandria-Wonarah Basement High. The generalised conceptual geochemical model for the transport and formation of secondary mineralisation at the 'supergene' and 'water intercept' zones is depicted. The zig-zags lines represent lateral transitions between hydrogeologically equivalent stratigraphic units (that are shown in Fig. 2). Also depicted are siltstone lenses that act as aquitards and inhibit vertical mixing of groundwater in the Barkly Sub-basin, as a potential explanation for observing less *Phos#* anomalies. Figure adapted from Dixon-Jain et al. (2024).

5.2. Understanding the Phos# Index

Given the empirical nature of *Phos#*, it's important to investigate the geological or geochemical basis to support these P* elemental relationships. The rationale for the element associations incorporated into the *Phos#* index is strengthened when considering that this secondary mineralisation is redox controlled and mediated by long-term groundwater transport. Pufahl and Groat (2017) note that Mo is one of several trace elements enriched in francolite, substituting for Ca or occupying interstitial sites. Additionally, Mo is a redox sensitive element that adsorbs strongly onto organic matter and metal oxides (the latter prevalent in secondary phosphate mineralisation), and is readily transported in oxic conditions (Smedley and Kinniburgh, 2017). Thus, the model for secondary phosphate mineralisation would explain both the co-occurrence of Mo (sourced from primary phosphate mineralisation), and the geochemical transport and trapping of Mo at these redox fronts.

We hypothesise several reasons for a weaker relationship of P* with Mo* in cluster 2b (Fig. 7b), despite the proximity of phosphate deposits within the Undilla Sub-basin. Samples within cluster 2b have a shorter flow path (given they are near the point of recharge and local groundwater divide), and are hosted in more karstic, high-flow aquifers (Dixon-Jain et al., 2024). These factors mean less capacity for WRI and thermodynamic equilibration of the groundwater with local phosphorites. Another consideration is the potential for Mo (associated with mineralisation) to be immobilised by high levels of organic matter. The absence of the clay-rich surface veneer of the Barkly Tablelands (black soils) in the Undilla Sub-basin may enable more infiltration of organic matter from low-density cattle farming (Jackson et al., 2023) and natural vegetation decay into the local aquifers compared with the rest of the basin. This is validated by intermittent periods of high organic matter in the groundwater in previous studies (Eberhard, 2003). Lastly, there is evidence for compartmentalised or distinct groundwater systems locally in the Undilla Sub-basin, with perched or hydrologically separate CLA aquifers (Eberhard, 2003). This likely means several of the samples are from groundwaters geochemically disconnected from neighbouring samples and missing the Mo* indicator of phosphate mineralisation.

The mechanism for I* being inversely proportional to P* is a more complicated one. Iodide is a conservative anion in aqueous solution, and does not have any common mineral sources, excepting substitution within evaporites/halite. Iodide is most commonly found adsorbed on organic material, illite and metal-(oxyhydr)oxides (Fuge and Johnson, 1986; Kaplan et al., 2000; Lloyd et al., 1982). Consequently, two processes are considered for explaining this inverse relationship. The first and most likely, is that given these secondary phosphorites are very low in I^-, WRIs are adding P to solution at a rate exceeding background evaporative enrichment and salinisation processes. Alternatively, as the proportion of P_2O_5 in the rock increases, the proportion of material that adsorb I^- decreases, though this is less likely given we would expect to see associated inverse relations of P* with Fe*-Al*-Mn* and/or $\delta^{13}C$. Care must be taken in extrapolating this relationship to other sedimentary phosphate systems without prior understanding of the local phosphorites, as Ren et al. (2015) noted that some phosphorites can be enriched in I^-, associated with biogenic (algae) enrichment processes during sedimentation.

The relationship of P* with Al* appears to capture different hydrogeological processes, as P* only has a correlation with Al* in cluster 3 (Table S1). This localised relationship is interpreted to be due to the higher siliciclastic (especially clay) content of sediments in the Barkly Sub-basin relative to the Central Georgina and Undilla Sub-basins, potentially in conjunction with infiltration of groundwater through the clay-rich regolith of the Barkly Tablelands. The association of P* with Al* in groundwater of this region is validated by the prevalence of supergene, Al-phosphate minerals (wavellite; $Al_3(PO_4)_2(OH,F)_3{\cdot}5H_2O$, and crandallite; $CaAl_3(PO_4)(PO_3OH)(OH)_6$) at the nearby Wonarah deposit (Lilley and Broadbent, 2002), as well as enriched whole-rock geochemistry P_2O_5 and Al_2O_3 observed in the 'supergene' and 'water-intercept' zones of the Alexandria-Wonarah Basement High (Schroder et al., 2024b). Thus, it is reasonable to conclude that the correlation of P* with Al* in cluster 3 is still an indicator of nearby phosphorites in the 'water intercept' zone, and is suggestive of phosphorites extending north and east of cluster 3 samples within the Barkly Sub-basin. However, due to the very low solubility of Al, the relationship of P* to Al* does not provide any insight into primary phosphate mineralisation sources and/or transport processes (in contrast to P* vs Mo*), meaning that the absence of a combined P* and Al* anomaly is not discriminatory for the presence of phosphate mineralisation.

Of the other elements that contribute to PC4 (also summarised in Table S1), P*'s inverse relationship with Rb* is similar to I*, but with more scatter in each cluster (Fig. S4). Given Rb is also a conservative element in solution, we think this is mirroring the relationship of P* with I*, with WRI (of phosphorites) exceeding evaporative enrichment. Greater scatter is observed in this inverse P* vs Rb* relationship, likely due to competing sources for Rb, such as WRI with K-rich minerals (such as illite and K-feldspar). To better understand the processes that are correlating these elements with P (and their spatial variability) further geochemical sampling of the host-rock, with specific focus on the deportment of elements from mineral chemistry would be required. Such a study should target both the enriched redox interfaces (the 'supergene' and 'water intercept' zones) as well as background sections of the CLA, to provide insights into which elements are more readily mobilised via WRIs and/or have confounding sources distinct from phosphorite mineralisation.

The clusters generated from this approach are not optimal for partitioning of NAHS-CLA samples to best capture P relationships with substituent or correlated elements. There is uncertainty associated with clustering data purely using hydrogeochemistry, both because the margins of each cluster can overlap or display similarity with adjacent clusters (Templ et al., 2008), and because the process does not factor in hydrogeological constraints. This is expected, given the hydrogeochemical model of enriched P being derived from up-flow (and hydrologically connected) phosphorites would be distinct from bulk hydrogeological controls that more strongly inform the definition of clusters. For example, several outlier samples in cluster 2b (Fig. 7a) align closely with cluster 5c, as well as being spatially adjacent to the cluster (and vice-versa). If these samples were reclassified into the other cluster, both clusters' linear P* vs Mo* relationships would improve. Additionally, approximately a quarter of cluster 3 samples are strongly undersaturated with respect to hydroxyapatite, and their removal greatly increases the observed elemental correlations with P* (Table S1).

The valid question of why no elevated *Phos#* were observed in groundwater samples from the Barkly Sub-basin (clusters 3 and 5a) remains, especially considering high P_2O_5 concentrations were observed in proximal drill core (Schroder et al., 2024a). Reviewing the bore and sample information for screen and pump depth information, we identified that the depth of the groundwater samples was typically >20 m below the water intercept zone (or standing water level). We suspect this offset would be a somewhat common occurrence across the CLA, since screens are typically installed below the first water intercept to accommodate changes in groundwater levels expected over the bore's lifetime. By itself, this depth offset shouldn't affect the propagation of a mineralisation signal to the screened interval, except in circumstances where vertical mixing of groundwater is restricted (Fig. 10). This happens to be the case for much of the CLA through the Alexandria-Wonarah Basement High and Barkly Sub-basin, with higher proportions of siliciclastic (and particularly siltstone) intervals compared with the Central Georgina and Undilla Sub-basins. These siltstone layers are local to regional aquitard lenses that restrict vertical mixing (Dixon-Jain et al., 2024; ELA, 2022), and are inferred to be inhibiting mixing and equilibration with high P groundwater from the 'water intercept' zone. In contrast, the Camooweal Dolostone and Gum Ridge Formation in the Central Georgina and Undilla Sub-basins are predominantly

karstic carbonates, which support greater vertical mixing (Dixon-Jain et al., 2024; Eberhard, 2003; Randal, 1978), and can propagate dissolved P away from the 'water intercept' zone to the screened depths.

5.3. Implications for exploration

Heterogeneity in aquifer composition and hydraulic properties are an inherent limitation of hydrogeochemistry when applied to exploration. When evaluating groundwater anomalies (such as those presented in Figs. 8 and 9) in an exploration context (Leybourne and Cameron, 2010), it is important to consider the groundwater recharge and flow pathways (as any anomaly points to an up-flow source). Equally, given the complex nature of hydrogeochemistry, there is a risk of any individual sample giving a false negative (or false positive) due to mixing, sampling a different aquifer, redox controls, or biases in sampling and analysis. To alleviate this, as demonstrated here, the interpretation of hydrogeochemical data needs thorough grounding in the local hydrogeology, and screening of samples to equivalent hydrostratigraphic units. In addition, the threshold for follow-up should require multiple spatially adjacent anomalies, meaning groundwater is, in most instances, best applied as a scale-reduction tool in an exploration program.

Sedimentary phosphate is an ideal mineral family to explore for using groundwater chemistry, given the aquifer geology is hosting the mineralisation, and multiple elements (in addition to P) can act as pathfinders for mineralisation. Here we demonstrated an approach using multivariate statistical analysis to identify empirical relationships of P with Mo and I^-, that was supported by insight into local secondary mineralisation and the interplay with hydrogeology. Before applying *Phos#* to groundwaters in other basins to assess phosphate prospectivity, we recommend a similar approach of considering what is known regarding the phosphate mineralisation in conjunction with multivariate compositional data analysis. In particular, the depositional, diagenetic and weathering processes that the phosphorites have undergone will influence the phosphate's texture and geochemistry (Zivak et al., 2024). This consideration may alter or add to the contributing elements to the index. For example, if a similar scenario were encountered, with groundwater mainly in contact with secondary mineralisation, other redox sensitive elements such as U or V would be more appropriate than Mo as an indicator (depending on the local geology). Conversely, if infiltration of groundwater through weathered phosphorites is suspected, then Al and Fe might be more relevant pathfinders. Where primary phosphate mineralisation is the prevalent source of P in groundwater, more conventional minor and trace elements that substitute in francolite (F^-, Se, Zn, Cu, Cr, U and REEs) may be more robust as mineralisation pathfinders (Pan and Fleet, 2002; Pufahl and Groat, 2017). An area that has potential to support vectoring towards phosphorites is Pb isotopes and REE patterns (Wang et al., 2023). The present study did not investigate deeply these approaches due to the lack of Pb isotopes from local phosphate deposits, and the low dissolved REE concentrations that frequently are below instrumental detection limits.

Similarly, sediment-hosted Zn–Pb is well placed to be explored for using groundwater, as the sedimentary aquifer can host both the mineralisation and the groundwater. Due to the low-solubility of Pb (and to a lesser extent, other indicator elements like Zn), Pb isotopes are the most widespread and discriminating tool for detecting and distinguishing base-metal mineralisation in groundwater (Caritat et al., 2005, Leybourne et al., 2009). Several areas are identified with outlier radiogenic Pb isotope character that are indicative of interaction with MVT mineralisation. The significance of these Pb isotope anomalies observed in groundwater and drillholes could be validated by comparison with regolith Pb isotopes (Desem et al., 2024) as well as further Pb isotope analysis in the Georgina Basin to characterise endmember compositions. In particular, the background whole-rock Pb isotope range for Georgina Basin lithologies across different parts of the basin needs further resolution, as well as the Pb isotope composition of the galena grains in the ET-NDI drillholes (Schofield et al., 2022; Schroder et al., 2024a), so these new mineralisation intercepts can be compared with other MVT deposits in the basin. Additionally, higher density groundwater sampling in the vicinity of these anomalies may yield insights into the direction of mineralisation (vectoring), as well as a better understanding of the down-flow distance that isotope and elemental anomalies can be expected to propagate in groundwater.

Lastly, it is worth investigating if there is a second independent indicator of sediment-hosted Zn–Pb in groundwater, given the limited usefulness of trace element concentrations for investigating base-metals in low-density groundwater surveys. One promising avenue is the application of other isotope systems, which is an actively growing area of research made possible with the improvement in analytical capabilities. Many potentially relevant isotope systems are being tested or have found early success when applied to mineral exploration, including Cu, Zn, Fe and Mo (Kidder et al., 2021; Mahan et al., 2023; Mathur and Wang, 2019).

6. Conclusions

By combining a multivariate analysis of groundwater geochemistry with local understanding of the Georgina Basin's hydrogeology and mineral systems, we identify multiple features that indicate prospectivity for sediment hosted Zn–Pb and phosphorites. Robust principal component analysis (rPCA) identified Mo and I^- (as well as Rb and Al) as elements partly correlated with the variance in P. K-means cluster analysis was able to identify clusters in the Alexandria-Wonarah Basement High, Central Georgina Sub-basin and Undilla Sub-basin where these relationships were strongest and led to the generation of *Phos#* – a geochemical index to identify the most prospective outliers in the hydrogeochemistry dataset indicative of nearby phosphorites. *Phos#* identified five areas with adjacent outlier samples. Three areas near Elliott are on the flanks of the outcropping Tomkinson Province, where no phosphorites have previously been encountered, while one area each was identified in the Central Georgina and Undilla Sub-basins. These latter two are bounded by known phosphorites, so there is an ongoing question as to whether these groundwater anomalies are associated with known phosphorites, or undiscovered mineralisation. However, given phosphorites on the Alexandria-Wonarah Basement High are interpreted as secondary redox-controlled phosphate accumulations, this model combined with these groundwater anomalies suggests there may be primary phosphorites still to be discovered deeper in the basin.

Groundwater compositions were also valuable for detecting regional sediment-hosted Zn–Pb mineralisation. It was not possible to employ multivariate statistical approaches due to the low concentrations of indicator metals (i.e. Cu, Pb, Zn). However, due to the radiogenic character of the basin's Mississippi Valley Type (MVT) mineralisation, Pb isotopes proved a powerful and prospective tool for suggesting areas in contact with mineralisation. Radiogenic Pb isotope outliers in the Alexandria-Wonarah Basement High and Undilla Sub-basin correlate spatially with nearby observed sulfides at surface or in drillholes and were partly supported by elevated Pb or Zn in groundwater. Although further work is recommended to constrain the local Pb isotope signature of Zn–Pb mineralisation (vs bedrock), and sample groundwater at higher density in these areas to validate these anomalies, our initial results are promising for identifying prospective undiscovered Zn–Pb mineralisation in the basin.

CRediT authorship contribution statement

Ivan Frederick Schroder: Writing – review & editing, Writing – original draft, Visualization, Validation, Software, Resources, Project administration, Methodology, Investigation, Formal analysis, Data curation, Conceptualization. **Patrice de Caritat:** Writing – review & editing, Supervision, Methodology, Investigation, Formal analysis, Data curation. **David Huston:** Writing – review & editing, Supervision, Investigation, Formal analysis. **David Champion:** Writing – review &

editing, Supervision, Methodology, Investigation, Formal analysis.

Declaration of competing interest

The authors declare that they have no known competing financial interests or personal relationships that could have appeared to influence the work reported in this paper.

Acknowledgements

Geoscience Australia acknowledges the traditional custodians of the country where this work was undertaken. This work was funded as part of Geoscience Australia's Exploring for the Future Program. We thank Dr. Roland Maas (University of Melbourne) for his efforts in achieving reliable Pb isotopes from such low-Pb groundwaters and rocks. We would like to acknowledge the Geoscience Australia laboratory staff for their support in preparing samples and conducting quality assurance and control of the results, as well as Geoscience Australia's cartography team for figure development. This manuscript was greatly improved through the constructive feedback of two anonymous reviewers, whom we extend our sincere thanks to.

Appendix 1

Geochemical species used in imputation. All elements/compounds from DO onward are expressed in mg/L.

T (°C), EC (μS/cm), Eh (mV), pH, DO (mg/L), S^{2-}, Fe^{2+}, HCO_3^-, Ca, K, Mg, Na, Cl^-, SO_4^{2-}, F^-, Br^-, I^-, NO_3^-, SiO_2, Al, As, B, Ba, Co, Cr, Cu, Fe, Ga, Ge, Li, Mn, Mo, Ni, P, Rb, Sc, Se, Sr, Ti, U, V, Zn, Zr.

Variables explanation:

- T (°C), temperature
- EC (μS/cm), electrical conductivity
- Eh (mV), measure of oxidation-reduction potential of groundwater
- pH, measure of acid-base character of groundwater (dimensionless)
- DO (mg/L), dissolved oxygen

Appendix 2

Species used in robust Principal Component Analysis (rPCA) (all in mg/L). Ca, K, Mg, Na, Cl^-, SO_4^{2-}, F^-, Br^-, I^-, SiO_2, Al, As, B, Ba, Cr, Cu, Ge, Li, Mn, Mo, P, Rb, Se, Sr, U, V, Zn, HCO_3^-.

Appendix 3. Supplementary data

Supplementary data to this article can be found online at https://doi.org/10.1016/j.gexplo.2025.107857.

Data availability

The data used in this study is freely available as Supplementary Material

References

Ariunbileg, S., Gaskova, O., Vladimirov, A., Battushig, A., Moroz, E., 2016. Spatial distribution of uranium and metalloids in groundwater near sandstone-type uranium deposits, Southern Mongolia. Geochemical Journal 50 (5), 393–401. https://doi.org/10.2343/geochemj.2.0434.

Bethke, C.M., Farrell, B., Sharifi, M., 2024. The Geochemist's Workbench® Release 17: GWB Essentials Guide. Aqueous Solutions LLC, Champaign, USA.

Buccianti, A., Grunsky, E., 2014. Compositional data analysis in geochemistry: are we sure to see what really occurs during natural processes? J. Geochem. Explor. 141, 1–5. https://doi.org/10.1016/j.gexplo.2014.03.022.

Campbell, N.A., 1980. Robust procedures in multivariate analysis I: robust covariance estimation. J. R. Stat. Soc.: Ser. C: Appl. Stat. 29 (3), 231–237. https://doi.org/10.2307/2346896.

Caritat, P. de, Kirste, D., 2005a. Hydrogeochemistry applied to mineral exploration under cover in the Curnamona Province. MESA Journal 37, 13–17.

Caritat, P. de, Kirste, D., 2005b. Using groundwater to vector towards mineralisation under cover: the Curnamona Province. In: Roach, I. (Ed.), Regolith 2005 – Ten Years of CRC LEME, pp. 32–34.

Caritat, P. de, Kirste, D., Carr, G., McCulloch, M., 2005. Groundwater in the Broken Hill region, Australia: recognising interaction with bedrock and mineralisation using S, Sr and Pb isotopes. Appl. Geochem. 20 (4), 767–787. https://doi.org/10.1016/j.apgeochem.2004.11.003.

Caritat, P. de, Bastrakov, E.N., Jaireth, S., English, P.M., Clarke, J.D.A., Mernagh, T.P., Wygralak, A.S., Dulfer, H.E., Trafford, J., 2019. Groundwater geochemistry, hydrogeology and potash mineral potential of the Lake Woods region, Northern Territory, Australia. Aust. J. Earth Sci. 66 (3), 411–430. https://doi.org/10.1080/08120099.2018.1543208.

Champion, D.C., Huston, D., Main, P., Jarrett, A.J.M., Thorne, J., Gilmore, S., Webber, S., Webster, T., Byass, J., DiBugnara, D., Williamson, A.D., Long, I., Peljo, N., 2020. Exploring for the Future – Baseline Whole Rock Geochemistry of Northern Australia: Data Release — Geochemistry of Drill Core Samples from the McArthur Basin, Lawn Hill Platform and Tomkinson Province, Northern Territory and Queensland. Record 2020/41. Geoscience Australia, Australia. https://doi.org/10.11636/Record.2020.041.

Cloutier, V., Lefebvre, R., Therrien, R., Savard, M.M., 2008. Multivariate statistical analysis of geochemical data as indicative of the hydrogeochemical evolution of groundwater in a sedimentary rock aquifer system. J. Hydrol. 353 (3–4), 294–313. https://doi.org/10.1016/j.jhydrol.2008.02.015.

Cloutier, J., Ford, A., Huston, D., Doublier, M., Schofield, A., Waltenberg, K., Caritat, P. de, Fraser, G., Beyer, E., Bastrakov, E., Czarnota, K., 2023. National Mineral Potential for Sediment-hosted Zinc-Lead Mineral Systems in Australia Version 1.0. Geoscience Australia, Australia. https://doi.org/10.26186/147540.

Cotter, S.J., Moore, C.L., Taylor, G., Prince, K.E., 2002. Isotopic constraints on large-scale Sedex or MVT mineralization within the Cambrian carbonate cover sequences, northwest Qld. In: Roach, I. (Ed.), Regolith and Landscapes in Eastern Australia, pp. 14–16.

Creveling, J.R., Johnston, D.T., Poulton, S.W., Kotrc, B., März, C., Schrag, D.P., Knoll, A. H., 2014. Phosphorus sources for phosphatic Cambrian carbonates. Bulletin 126 (1-2), 145–163. https://doi.org/10.1130/B30819.1.

Critical Minerals Office, 2024. Australia's critical minerals list and strategic materials list. https://www.industry.gov.au/publications/australias-critical-minerals-list-and-strategic-materials-list.

Crosbie, R., Morrow, D., Cresswell, R., Leaney, F., Lamontagne, S., Lefournour, M., 2012. New insights to the chemical and isotopic composition of rainfall across Australia. In: EP125581; CSIRO Water for a Healthy Country Flagship, Australia. https://doi.org/10.5072/83/5849a0d6c685a.

Desem, C.U., Caritat, P. de, Woodhead, J., Maas, R., Carr, G., 2024. A regolith lead isoscape of Australia. Earth System Science Data 16 (3), 1383–1393. https://doi.org/10.5194/essd-16-1383-2024.

Deslandes, A., Gerber, C., Lamontagne, S., Wilske, C., Suckow, A., 2019. Environmental Tracers in the Beetaloo Basin. Aquifer and Groundwater Characterization. EP198539. CSIRO, Australia. http://hdl.handle.net/102.100.100/385078?index=1.

Dixon-Jain, P., Bishop, C., Lester, J., Orlov, C., McPherson, A., Pho, G., Flower, C., Kilgour, P., Lawson, S., Vizy, J., Lewis, S., 2024. Hydrogeology and Groundwater Systems of the South Nicholson and Georgina Basins, Northern Territory and Queensland. *Record 2024/37*. Geoscience Australia, Australia. https://doi.org/10.26186/149730.

Drever, J.I., 1997. The Geochemistry of Natural Waters: Surface and Groundwater Environments, 3rd ed. Prentice Hall, New Jersey, USA.

Dunster, J., Munson, T., 2017. Georgina Basin phosphate deposits. In: Phillips, G. (Ed.), Australian Ore Deposits. AusIMM, Melbourne, Australia, p. 864.

Dunster, J., Kruse, P., Duffett, M., Ambrose, G., 2007. Geology and Resource Potential of the Southern Georgina Basin: GIS Package and Report. Report DIP007. Northern Territory Geological Survey, Australia. https://geoscience.nt.gov.au/gemis/ntgsjspui/handle/1/81746.

Eberhard, S., 2003. Nowranie caves and the Camooweal karst area, Queensland. Helictite 38 (2), 27–38.

Egozcue, J.J., Gozzi, C., Buccianti, A., Pawlowsky-Glahn, V., 2024. Exploring geochemical data using compositional techniques: a practical guide. J. Geochem. Explor. 258, 107385. https://doi.org/10.1016/j.gexplo.2024.107385.

ELA, 2022. Strategic regional environmental and baseline assessment for the Beetaloo Sub-basin: water quality and quantity baseline summary report. Technical Report 24/2022. In: Report Prepared for the Northern Territory Department of Environment, Parks and Water Security by Eco Logical Australia (ELA) and Tetra Tech Coffey.

Elango, L., Kannan, R., 2007. Rock–water interaction and its control on chemical composition of groundwater. Developments in environmental science 5, 229–243. https://doi.org/10.1016/S1474-8177(07)05011-5.

Fuge, R., Johnson, C.C., 1986. The geochemistry of iodine — a review. Environ. Geochem. Health 8, 31–54. https://doi.org/10.1007/BF02311063.

Gallagher, V., Grunsky, E.C., Fitzsimons, M.M., Browne, M.A., Lilburn, S., Symons, J., 2022. Tellus regional stream water geochemistry: environmental and mineral exploration applications. Geochemistry: Exploration, Environment, Analysis 22 (1). https://doi.org/10.1144/geochem2021-050.

Geoscience Australia, 2020. Mineral Deposits and Mineral Resources WMS. Geoscience Australia, Australia. https://pid.geoscience.gov.au/dataset/ga/144671.

Gray, D.J., Reid, N., Noble, R.R.P., 2014. Improved hydrogeochemical exploration in the northwest Yilgarn – adding value to underexplored areas. In: EP143875. CSIRO, Australia. https://doi.org/10.4225/08/5858207ec0902.

Gray, D.J., Yeats, C.J., Noble, R.R.P., Reid, N., 2018. Hydrogeochemical exploration for volcanic-hosted massive sulfide deposits in semi-arid Australia. Aust. J. Earth Sci. 65 (2), 249–274. https://doi.org/10.1080/08120099.2018.1423110.

Grunsky, E.C., 2010. The interpretation of geochemical survey data. Geochemistry: Exploration, Environment, Analysis 10 (1), 27–74. https://doi.org/10.1144/1467-7873/09-210.

Grunsky, E.C., Caritat, P. de, 2020. State-of-the-art analysis of geochemical data for mineral exploration. Geochemistry: Exploration, Environment, Analysis 20 (2), 217–232. https://doi.org/10.1144/geochem2019-031.

Güler, C., Thyne, G.D., McCray, J.E., Turner, K.A., 2002. Evaluation of graphical and multivariate statistical methods for classification of water chemistry data. Hydrogeol. J. 10, 455–474. https://doi.org/10.1007/s10040-002-0196-6.

Hill, R.C., Wang, Z., Williams, G.D., Polyak, V., Singh, A., Kipp, M.A., Asmerom, Y., Vengosh, A., 2024. Reconstructing the depositional environment and diagenetic modification of global phosphate deposits through integration of uranium and strontium isotopes. Chem. Geol. 662. https://doi.org/10.1016/j.chemgeo.2024.122214.

Hron, K., Templ, M., Filzmoser, P., 2010. Imputation of missing values for compositional data using classical and robust methods. Computational Statistics and Data Analysis 54 (12), 3095–3107. https://doi.org/10.1016/j.csda.2009.11.023.

Hughes, A., Britt, A., Pheeney, J., Morfiadakis, A., Kucka, C., Colclough, H., Munns, C., Senior, A., Cross, A., Hitchman, A., Cheng, Y., Walsh, J., Jayasekara, A., 2025. Australia's Identified Mineral Resources 2024. Geoscience Australia, Australia. https://doi.org/10.26186/149861.

Huston, D.L., Champion, D.C., 2023. Applications of lead isotopes to ore geology, metallogenesis and exploration. In: Huston, D., Gutzmer, J. (Eds.), Isotopes in Economic Geology, Metallogenesis and Exploration. Mineral Resource Reviews. Springer, USA. https://doi.org/10.1007/978-3-031-27897-6_6.

Huston, D.L., Champion, D.C., Ware, B., Carr, G., Maas, R., Tessalina, S., 2019. Preliminary National-scale Lead Isotope Maps of Australia. Record 2019/001. Geoscience Australia, Australia. https://doi.org/10.11636/Record.2019.001.

Jackson, D., Dixon, R., Quigley, S., Schatz, T., Rolfe, J., Corbett, E., English, B., Sullivan, M., Chudleigh, F., Wellinton, M., Callaghan, M., 2023. In: Perry, L. (Ed.), Phosphorus Management of Beef Cattle in Northern Australia, 2nd edition. Meat and Livestock Australia Limited, Australia.

Kaplan, D.I., Serne, R.J., Parker, K.E., Kutnyakov, I.V., 2000. Iodide sorption to subsurface sediments and illitic minerals. Environ. Sci. Technol. 34 (3), 399–405. https://doi.org/10.1021/es990220g.

Kidder, J.A., Voinot, A., Leybourne, M.I., Layton-Matthews, D., Bowell, R.J., 2021. Using stable isotopes of Cu, Mo, S, and $^{87}Sr/^{86}Sr$ in hydrogeochemical mineral exploration as tracers of porphyry and exotic copper deposits. Appl. Geochem. 128. https://doi.org/10.1016/j.apgeochem.2021.104935.

Kidder, J.A., McClenaghan, M.B., Leybourne, M.I., McCurdy, M.W., Pelchat, P., Layton-Matthews, D., Voinot, A., 2022. Hydrogeochemistry of porphyry-related solutes in ground and surface waters; an example from the Casino Cu–Au–Mo deposit, Yukon, Canada. Geochem.: Explor., Environ., Anal. 22(2), 2021–2058. https://doi.org/10.1144/geochem2021-058.

Kruse, P., Dunster, J., Munson, T., 2013. Chapter 28: Georgina Basin. In: Ahmad, M., Munson, T. (Eds.), Geology and Mineral Resources of the Northern Territory. Northern Territory Geological Survey, Australia.

Leybourne, M.I., Cameron, E.M., 2010. Groundwater in geochemical exploration. Geochem.: Explor., Environ., Anal. 10, 99–118. https://doi.org/10.1144/1467-7873/09-222.

Leybourne, M.I., Cousens, B.L., Goodfellow, W.D., 2009. Lead isotopes in ground and surface waters: fingerprinting heavy metal sources in mineral exploration. Geochem.: Explor., Environ., Anal. 9 (2), 115–123. https://doi.org/10.1144/1467-7873/09-195.

Lilley, G.L., Broadbent, G.C., 2002. Combined Annual Report for the Period Ending 31/07/02 EL9976, EL22167, and EL22168 Wonarah, Northern Territory. Report No. 25490;. Rio Tinto Exploration Pty. Ltd.

Lloyd, J.W., Howard, K.W.F., Pacey, N.R., Tellam, J.H., 1982. The value of iodide as a parameter in the chemical characterisation of groundwaters. J. Hydrol. 57 (3–4), 247–265. https://doi.org/10.1016/0022-1694(82)90149-4.

Mahan, B., Mathur, R., Sanislav, I., Rea, P., Dirks, P., 2023. Cu isotopes in groundwater for hydrogeochemical mineral exploration: a case study using the world-class Mount Isa Cu–Pb–Zn deposit (Australia). Appl. Geochem. 148. https://doi.org/10.1016/j.apgeochem.2022.105519.

Mathur, R., Wang, D., 2019. Chapter 7: Transition metal isotopes applied to exploration geochemistry: insights from Fe, Cu, and Zn. In: Decrée, S., Robb, L. (Eds.), Ore Deposits: Origin, Exploration, and Exploitation. Geophysical Monograph Series, USA. https://doi.org/10.1002/9781119290544.ch7.

Mathur, R., Zhao, Y., 2023. Copper isotopes used in mineral exploration. In: Huston, D., Gutzmer, J. (Eds.), Isotopes in Economic Geology, Metallogenesis and Exploration. Mineral Resource Reviews. Springer, USA. https://doi.org/10.1007/978-3-031-27897-6_14.

Moya, C.E., Raiber, M., Taulis, M., Cox, M.E., 2016. Using environmental isotopes and dissolved methane concentrations to constrain hydrochemical processes and inter-aquifer mixing in the Galilee and Eromanga Basins, Great Artesian Basin, Australia. J. Hydrol. 539, 304–318. https://doi.org/10.1016/j.jhydrol.2016.05.016.

Oelkers, E.H., Benezeth, P., Pokrovski, G.S., 2009. Thermodynamic databases for water-rock interaction. Rev. Mineral. Geochem. 70 (1), 1–46. https://doi.org/10.2138/rmg.2009.70.1.

O'Shea, B., Jankowski, J., 2006. Detecting subtle hydrochemical anomalies with multivariate statistics: an example from 'homogeneous' groundwaters in the Great Artesian Basin, Australia. Hydrological Processes: An International Journal 20 (20), 4317–4333. https://doi.org/10.1002/hyp.6177.

Pan, Y., Fleet, M.E., 2002. Compositions of the apatite-group minerals: substitution mechanisms and controlling factors. Rev. Mineral. Geochem. 48 (1), 13–49. https://doi.org/10.2138/rmg.2002.48.2.

Piper, A.M., 1944. A graphic procedure in the geochemical interpretation of water-analyses. EOS Trans. Am. Geophys. Union 25 (6), 914–928. https://doi.org/10.1029/TR025i006p00914.

Pufahl, P.K., Groat, L.A., 2017. Sedimentary and igneous phosphate deposits: formation and exploration: an invited paper. Econ. Geol. 112 (3), 483–516. https://doi.org/10.2113/econgeo.112.3.483.

Randal, M.A., 1978. Hydrogeology of the Southeastern Georgina Basin and Environs, Queensland and Northern Territory. Publication 366. Geological Survey of Queensland, Australia.

Reid, N., Thorne, R., Folkes, C., Gilmore, P.J., Pinchand, T., 2021. Hydrogeochemistry of the Cobar Region. EP 207556; CSIRO, Australia. Record GS2021/0054. Geological Survey of New South Wales, Australia. https://doi.org/10.25919/fv9r-zk57.

Ren, H., Yang, R., Gao, J., Cheng, W., Wei, H., 2015. Enrichment regularities for iodine concentration in phosphorite of Doushantuo Formation of late Ediacaran in Guizhou Province, SW China. Arab. J. Geosci. 8, 5423–5437. https://doi.org/10.1007/s12517-014-1604-7.

Sahai, N., Schoonen, M.A., 2020. Accuracy of thermodynamic databases for hydroxyapatite dissolution constant. Astrobiology 20 (1), 157–160. https://doi.org/10.1089/ast.2019.2158.

Schofield, A., Clark, A., Kositcin, N., Cross, A., Doublier, M., Skirrow, R., Fraser, G., Budd, A., Close, D.F., Jiang, W., Murr, J., O'Rourke, A., Pitt, L., Roach, I., Thomas, M., Whelan, J.A., Wynne, P., 2022. Shining New Light on the (Previously) Dark Depths of the East Tennant Region. AGES 2022 extended abstract. https://geoscience.nt.gov.au/gemis/ntgsjspui/handle/1/92073.

Schroder, I., Caritat, P. de, Wallace, L., Tobin, J., Boreham, C., English, P., Sohn, J., Palatty, P., Coghlan, R., Maher, P., Thorose, M.D., Long, I., Byass, J., Jinadasa, N., 2020. Northern Australia Hydrogeochemical Survey: Final Data Release and Atlas for Exploring for the Future. Record 2020/015. Geoscience Australia, Australia. https://doi.org/10.11636/Record.2020.015.

Schroder, I.F., Caritat, P. de, Schofield, A., Champion, D.C., 2024a. Rock geochemistry and isotopes from the Georgina Basin. Exploring for the Future – East Tennant NDI drillholes. *Record 2024/04*. Geoscience Australia, Australia. https://doi.org/10.26186/148954.

Schroder, I.F., Huston, D., Caritat, P. de, 2024b. The geochemistry of redox interfaces for insights into Zn-Pb prospectivity in the Georgina Basin. In: Czarnota, K. (Ed.), Exploring for the Future: Extended Abstracts. Geoscience Australia, Australia. https://doi.org/10.26186/149116.

Smedley, P.L., Kinniburgh, D.G., 2017. Molybdenum in natural waters: a review of occurrence, distributions and controls. Appl. Geochem. 84, 387–432. https://doi.org/10.1016/j.apgeochem.2017.05.008.

Tao, Y., Du, Y., Deng, Y., Huang, Y., Leng, Z., Ma, T., Wang, Y., 2022. Carbon and iron isotope approach elucidates the enrichment of geogenic phosphorus in alluvial-lacustrine sedimentary aquifers. J. Hydrol. 607. https://doi.org/10.1016/j.jhydrol.2022.127517.

Templ, M., Filzmoser, P., Reimann, C., 2008. Cluster analysis applied to regional geochemical data: problems and possibilities. Appl. Geochem. 23 (8), 2198–2213. https://doi.org/10.1016/j.apgeochem.2008.03.004.

Templ, M., Hron, K., Filzmoser, P., Gardlo, A., 2016. Imputation of rounded zeros for high-dimensional compositional data. Chemom. Intell. Lab. Syst. 155, 183–190. https://doi.org/10.1016/j.chemolab.2016.04.011.

Tickell, S.J., Bruwer, Q., 2017. Georgina Basin groundwater assessment: Daly Waters to Tennant Creek. In: Report 17/2017 (Version 2, April 2019). Australia, Northern Territory Department of Environment and Natural Resources.

Tukey, J.W., 1977. Exploratory Data Analysis, Vol 2. Addison-Wesely, United Kingdom.

Vaasjoki, M., Gulson, B.L., 1986. Carbonate-hosted base metal deposits; lead isotope data bearing on their genesis and exploration. Econ. Geol. 81 (1), 156–172. https://doi.org/10.2113/gsecongeo.81.1.156.

Valetich, M., Zivak, D., Spandler, C., Degeling, H., Grigorescu, M., 2022. REE enrichment of phosphorites: an example of the Cambrian Georgina Basin of Australia. Chem. Geol. 588. https://doi.org/10.1016/j.chemgeo.2021.120654.

Walter, J., Chesnaux, R., Cloutier, V., Gaboury, D., 2017. The influence of water/rock–water/clay interactions and mixing in the salinization processes of groundwater. Journal of Hydrology: Regional Studies 13, 168–188. https://doi.org/10.1016/j.ejrh.2017.07.004.

Wang, Z., Hill, R., Williams, G., Dwyer, G.S., Hu, J., Schnug, E., Bol, R., Sun, Y., Coleman, D.S., Liu, X.M., Sandstrom, M.R., 2023. Lead isotopes and rare earth elements geochemistry of global phosphate rocks: Insights into depositional conditions and environmental tracing. Chem. Geol. 639. https://doi.org/10.1016/j.chemgeo.2023.121715.

Ware, B.D., Jourdan, F., Merle, R., Chiaradia, M., Hodges, K., 2018. The Kalkarindji Large Igneous Province, Australia: petrogenesis of the oldest and most compositionally homogenous province of the Phanerozoic. J. Petrol. 59 (4), 635–665. https://doi.org/10.1093/petrology/egy040.

Wilkinson, J., 2013. Sediment-hosted zinc-lead mineralization: processes and perspectives: processes and perspectives. In: Holland, K.T.H. (Ed.), Treatise on Geochemistry. Elselvier, United Kingdom. https://doi.org/10.1016/B978-0-08-095975-7.01109-8.

Zhang, X., Qian, H., Chen, J., Qiao, L., 2014. Assessment of groundwater chemistry and status in a heavily used semi-arid region with multivariate statistical analysis. Water 6 (8), 2212–2232. https://doi.org/10.3390/w6082212.

Zivak, D., Spandler, C., Valetich, M., 2024. Geochemical and isotopic (Nd, Sr) tracing of the origin of REE enrichment in the Cambrian Georgina Basin phosphorites. Geochem. Geophys. Geosyst. 25 (2). https://doi.org/10.1029/2023GC011207.

Zuo, R., Wang, J., Xiong, Y., Wang, Z., 2021. The processing methods of geochemical exploration data: past, present, and future. Appl. Geochem. 132. https://doi.org/10.1016/j.apgeochem.2021.105072.